
On Mitigating Random and Adversarial Bit Errors

David Stutz¹ Nandhini Chandramoorthy² Matthias Hein³ Bernt Schiele¹

¹ Max Planck Institute for Informatics, Saarland Informatics Campus

² IBM T. J. Watson Research Center ³ University of Tübingen

{david.stutz,schiele}@mpi-inf.mpg.de

nandhini.chandramoorthy@ibm.com matthias.hein@uni-tuebingen.de

Abstract

The design of deep neural network (DNN) accelerators, i.e., specialized hardware for inference, has received considerable attention in past years due to saved cost, area, and energy compared to mainstream hardware. We consider the problem of **random and adversarial bit errors in quantized DNN weights** stored on accelerator memory. Random bit errors arise when optimizing accelerators for energy efficiency by operating at low voltage. Here, the bit error rate increases exponentially with voltage reduction, causing devastating accuracy drops in DNNs. Additionally, recent work demonstrates attacks on voltage controllers to adversarially reduce voltage. Adversarial bit errors have been shown to be realistic through attacks targeting individual bits in accelerator memory. Besides describing these error models in detail, we make first steps towards DNNs robust to random and adversarial bit errors by explicitly taking bit errors into account during training. Our *random or adversarial bit error training* improves robustness significantly, potentially leading to more energy-efficient and secure DNN accelerators.

1 Introduction

The success of deep neural networks (DNNs) is partly due to parallel hardware, such as mainstream GPUs. Recently, *DNN accelerators*, i.e., specialized hardware for inference, have been used to reduce and limit energy consumption alongside cost and space. In particular, accelerators make use of highly parallel computational units, reduced precision, as well as custom memory organization and data flow to improve energy efficiency, e.g., see [1, 2, 3, 4, 5]. Low voltage operation is an effective strategy to lower energy consumption significantly. However, low voltage operation can lead to bit-level failures in memory [6, 7]. Additionally, recent work demonstrated severe security threats by intentionally manipulating operating voltage [8], or explicitly injecting bit errors in memory [9] to reduce DNN accuracy [10]. Such hardware related design and security constraints are typically not taken into account in DNN design. Obtaining *robustness against random or adversarial bit errors in quantized DNN weights* presents a challenging and unique problem for the machine learning community with direct impact on energy consumption and security of DNN accelerators.

DNN accelerators generally feature on-chip SRAM memory arrays used as scratchpads to store weights and inputs. In order to reduce energy consumption, operating voltage is reduced below V_{\min} , the minimum voltage at which error-free operation is guaranteed. This “low-voltage” operation causes bit failures in SRAMs with devastating effect on DNN accuracy. The rate p of bit errors is shown to increase exponentially as supply voltage is scaled down [6, 11, 12, 13]. For example, Fig. 1 (left) shows that obtaining robustness against, e.g., $p = 1\%$ bit errors at $0.83V_{\min}$ has the potential to reduce SRAM energy by roughly 30% compared to operation at V_{\min} . Circuit techniques such as error detection via redundancy [14] and supply voltage boosting [13] have been explored to guarantee robust DNN operation below V_{\min} . Such approaches allow significant reduction in energy, however, there is still an energy overhead incurred due to error mitigation in hardware. Therefore, [12, 15] trained DNNs robust to low-voltage induced SRAM and DRAM errors, respectively, by injecting

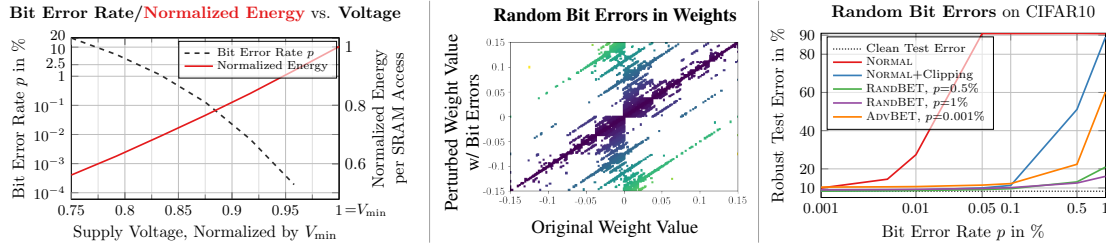


Figure 1: **Impact and Energy-Savings of Random Bit Errors.** *Left:* Exemplary SRAM bit error rate p and normalized energy per SRAM access [13], which has large impact on accelerator energy consumption as supply voltage is scaled below V_{\min} . *Middle:* Original weight value, quantized with 16 bits in $[-0.15, 0.15]$ on CIFAR10, plotted against the weight with random bit errors of rate $p = 1\%$; 5.5M weights shown. Color indicates error magnitude: zero (diagonal, violet) to ~ 0.225 (yellow). *Right:* Impact of bit errors on test error for CIFAR10. Reducing quantization range, i.e., clipping, to $[-0.15, 0.15]$ and random bit error training (RANDBET) clearly improves robustness.

profiled bit errors during training, i.e., chip-specific spatial distributions of bit failures in memory arrays. Thus, for every chip and operating voltage, the memory needs to be profiled and the DNNs need to be re-trained, both of which are not scalable.

Only few works consider robustness of DNNs in terms of quantized weights. In [16], the authors consider Gaussian noise on weights and, in [17, 18, 19, 20], the robustness of DNNs towards quantization is studied. Weng et al. [21] consider adversarial L_∞ perturbations on weights, also with an application to quantization. However, as shown in Fig. 1 (middle), bit errors represent a unique and challenging noise model where few bit errors, e.g., in the most significant bits (MSBs) can induce large changes. This is in stark contrast to Gaussian, L_∞ or quantization noise. Thus, the authors of [10] directly identify and adversarially flip bits in quantized weights to reduce accuracy. In concurrent work, He et al. [22] argue that training on such adversarially injected bit errors does not improve robustness and propose a binarization approach instead. In contrast, we demonstrate an adversarial bit error training technique that improves robustness and additionally consider the more realistic case of random bit errors, crucial for energy efficiency *and* security in DNN accelerators. Similar to [10], we do *not* provide an end-to-end demonstration of a security attack with adversarial bit flips on memory. Instead we identify and train on adversarial bit errors to improve robustness.

Contributions: We consider the problem of random and adversarial bit errors in DNN weights with fixed-point quantization. We demonstrate that random bit errors can cause severe drops in accuracy and adversarial bit errors are able to devastate accuracy with only few, but specific, bit flips. We incorporate completely random bit errors into the training procedure, resulting in robust operation across multiple bit error patterns and multiple voltage operating points. Furthermore, we present a min-max formulation of training with adversarial bit errors, resulting in significantly improved robustness against adversarially-induced bit failures, e.g., via attacks demonstrated in [9], as well as random bit errors caused by maliciously reducing operating voltage, as demonstrated in [8]. On MNIST [23], Fashion-MNIST [24] and CIFAR10 [25], we present extensive experiments showing that our approach leads to more secure *and* energy-efficient DNN accelerators.

2 Related work

Weight Robustness: Few works explicitly consider robustness to weight perturbations: [21] certify the robustness of weights with respect to L_∞ perturbations and [16] study Gaussian noise on weights. More related to our work, [10] considers identifying and flipping few vulnerable bits in quantized weights. In concurrent work, He et al. [22] propose a binarization approach to obtain robustness against such adversarial bit errors. Moreover, they argue that training with adversarial bit errors does *not* lead to improved robustness. Several works [17, 18, 19, 20] also consider the robustness of DNNs against quantization errors. Fault tolerance, in contrast, describes structural changes such as removed units, and is rooted in early work such as [26, 27] utilizing approaches similar to adversarial training [28]. Finally, some works [29, 30] explicitly manipulate weights in order to integrate backdoors. In contrast to [21, 16], we study robustness against random and adversarial *bit errors*. In contrast to [10], we propose a projected gradient ascent approach to obtain adversarial bit flips. And despite [22], we show that our adversarial bit attack allows a min-max training formulation, similar to [28], that improves robustness significantly. While we also consider fixed-point quantization [31, 32, 33], quantization errors are significantly less severe than bit errors.

Bit Errors in DNN Accelerators: Recent work [6, 11] demonstrates that bit flips in SRAMs increase exponentially when reducing voltage below V_{\min} . The authors of [13] study the impact of bit flips in different layers of DNNs, showing severe accuracy degradation. Similar observations hold for DRAM [34]. To prevent accuracy drops at low voltages, Minerva [14] combines SRAM fault detection with logic to set faulty data reads from the SRAM to zero when faults are detected. [13] uses supply voltage boosting for SRAMs to achieve robustness at low voltages, while [35] proposes storing critical bits in specifically robust SRAM cells. However, such methods incur power and area overhead. Thus, [12] injects profiled SRAM bit errors during training and [15] trains with DRAM errors and maps the model to DRAM in a way to guarantee a certain accuracy. Besides low-voltage operation for energy efficiency, recent work [8] shows that an attacker can reduce voltage maliciously. Similarly, works such as [36, 9] demonstrate software-based approaches to induce few, but targeted, bit flips in DRAM. Our bit error training improves robustness against random or adversarial bit errors and, in contrast to [12], generalizes across chips with different memory bit error patterns.

3 Random and Adversarial Bit Errors in Quantized DNNs

We consider two bit error models: First, random bit errors occur due to low voltage operation. Here, bit flips occur with probability p (in %). Second, we consider adversarial bit errors as motivated by recent attacks on memory [36, 9, 10]. In this setting, we consider a fixed budget of bit errors, e.g., a maximum of $p\%$ of bits can be flipped.

Notation: The DNN f predicts a probability distribution $f(x; w) \in \mathbb{R}^K$ for an input $x \in [0, 1]^D$ and weights $w \in [-w_{\max}, w_{\max}]^W$, where W is the total number of weights of the network. Given an input x and label y , the prediction is correct iff $y = \text{argmax}_k f_k(x; w)$. The DNN is trained by minimizing the cross-entropy loss \mathcal{L} . For quantized DNNs, m denotes the number of bits per weight value and Q is a quantization function such that $v := Q(w)$ denotes the quantized weight vector. In practice, v_i is a m -bit signed integer representing the underlying m bits. In the following, we use $v_i \in \{-2^{m-1}, \dots, 2^{m-1} - 1\}$ corresponding to the underlying bits $v_i \in \{0, 1\}^m$. De-quantization is expressed as $w_q := Q^{-1}(v)$. By $\tilde{v} = \text{BErr}_p(v)$, we denote random bit errors with probability p . On expectation, \tilde{v} has pmW bits flipped compared to v , as measured using the *bit-level* Hamming distance between m -bit signed integers $d_H(\tilde{v}, v)$.

Fixed-Point Quantization: Quantization determines how weights $w \in \mathbb{R}^W$ are represented, e.g., in SRAM. Following related work [31, 32, 33], we consider a *fixed-point quantization*: m bits allow to represent 2^m distinct values. For an arbitrary but fixed maximum absolute weight w_{\max} , the range $[-w_{\max}, w_{\max}]$ is quantized into bins of width Δ . We consider a quantized weight w_i to be represented by a signed m -bit integer $v_i = Q(w_i)$ (in two's complement representation) corresponding to the underlying bits. Then, $Q : \mathbb{R} \mapsto \{-2^{m-1}, \dots, 2^{m-1} - 1\}$ is defined as

$$Q(w) = \left\lfloor \frac{\max(-w_{\max}, \min(w_{\max}, w))}{\Delta} \right\rfloor, \quad Q^{-1}(v) = v\Delta \quad \text{with} \quad \Delta = \frac{w_{\max}}{2^{m-1} - 1}. \quad (1)$$

with element-wise operations. We emphasize, that quantization includes clipping the weights to $[-w_{\max}, w_{\max}]$. We do not quantize activations or gradients as, e.g., in [37, 38, 39, 40, 41, 42].

Low-Voltage Induced Random Bit Errors: Following [6, 12, 13], the probability of SRAM bit cell failures increases exponentially as operating voltage is scaled below V_{\min} , i.e., the minimal voltage required for reliable operation, see Fig. 1 (left). This is done intentionally to reduce energy consumption, e.g., [13, 12, 15], or adversarially by an attacker, e.g., [8]. Process variation during fabrication causes a variation in the extent of vulnerability of individual bit cells. For a given memory array, bit cell failures are assumed to be random and independent of each other, and there is a fixed spatial distribution of bit cell failures. As shown in [11], if a bit error occurred at a given voltage, it is likely to occur at lower voltages, as well. Across different SRAM arrays in a chip or different chips, the patterns or spatial distribution of bit errors is usually different and can be assumed random [13]. We condense these observations into the following bit error model used throughout the paper:

The probability of a bit error is p (in %) for all weight values and bits. For a fixed chip, bit errors are persistent across supply voltages, i.e., bit errors at probability $p' \leq p$ also occur at probability p . A bit error flips the currently stored bit. We denote random bit error injection by BErr_p .

We assume the quantized weights are stored linearly within the memory. Thus, in practice, for W weights and m bits per weight value, we sample uniformly $u \sim U(0, 1)^{W \times m}$. Then, the j -th bit in

Algorithm 1 Adversarial Bit Errors and Training. *Left:* We maximize cross-entropy loss using projected gradient ascent while ensuring that at most $\epsilon := \lceil pmW \rceil$ bits are flipped (W weight values, m bits each). Line 9 may include backtracking and Line 7 may include gradient normalization. *Right:* Our average-gradient adversarial weight training using adversarial bit errors or random bit errors. For illustration, we color the **original floating-point weights w in magenta**, the **quantized weights as signed m -bit integers $v = Q(w)$ in red** and the **de-quantized weights $w_q = Q^{-1}(v)$ in blue**.

<pre> 1: procedure ADVBITERRORS(w, p) 2: $v = Q(w)$, $\epsilon = \lceil pmW \rceil$ 3: initialize: $d_H(\tilde{v}^{(0)}, v) \leq \epsilon$, $d_H(\tilde{v}_i^{(0)}, v_i) \leq 1$ 4: for $t = 0, \dots, T-1$ do {fixed $\{(x_b, y_b)\}_{b=1}^B\}$ 5: $\tilde{w}_q^{(t)} = Q^{-1}(\tilde{v}^{(t)})$ 6: {forward pass using de-quantized weights:} 7: $\Delta^{(t)} = \nabla_w \sum_{b=1}^B \mathcal{L}(f(x_b; \tilde{w}_q^{(t)}), y_b)$ 8: {update without quantization:} 9: $\tilde{w}^{(t+1)} = \tilde{w}^{(t)} + \gamma \Delta^{(t)}$ 10: $\tilde{v}^{(t+1)} = Q(\tilde{w}^{(t+1)})$ 11: project: $d_H(\tilde{v}^{(t+1)}, v) \leq \epsilon$, $d_H(\tilde{v}_i^{(t+1)}, v_i) \leq 1$ 12: return $\tilde{w}_q^{(T)} = Q^{-1}(Q(\tilde{w}^{(T)}))$ </pre>	<pre> 1: procedure ADVBITERRORTRAINING(p) 2: initialize $w^{(0)}$ 3: for $t = 0, \dots, T-1$ do 4: sample batch $\{(x_b, y_b)\}_{b=1}^B$ 5: $w_q^{(t)} = Q^{-1}(Q(w^{(t)}))$ 6: $\Delta^{(t)} = \nabla_w \sum_{b=1}^B \mathcal{L}(f(x_b; w_q^{(t)}), y_b)$ 7: {inject adversarial or random bit errors:} 8: $\tilde{w}_q^{(t)} = \text{ADVBITERRORS}(w_q^{(t)}, p)$ {or BErr_p} 9: $\tilde{\Delta}^{(t)} = \nabla_w \sum_{b=1}^B \mathcal{L}(f(x_b; \tilde{w}_q^{(t)}), y_b)$ 10: clip $\Delta^{(t)}$ and $\tilde{\Delta}^{(t)}$ 11: $w^{(t+1)} = w^{(t)} - \gamma(\lambda \Delta^{(t)} + \tilde{\Delta}^{(t)})$ 12: return $w_q^{(T)} = Q^{-1}(Q(w^{(T)}))$ </pre>
---	---

the quantized weight $v_i = Q(w_i)$ is flipped iff $u_{ij} \leq p$. Our model assumes that the flipped bits at lower probability $p' \leq p$ are a subset of the flipped bits at probability p and that bit flips to 1 and 0 are equally likely. The unique noise pattern of random bit errors is illustrated in Fig. 1 (middle): for example a single bit flip in the most-significant bit (MSB) of the signed integer v_i can result in a change of roughly half of the quantized range, i.e., $\pm w_{\max}$.

Adversarial Bit Errors: Following recent attacks on memory [36, 43, 9, 10], we also consider adversarial bit errors. We constrain the number of induced bit errors by $\epsilon := \lceil pmW \rceil$, similar to the L_p -constrained adversarial inputs. Furthermore, we consider only one bit flip per weight value to simplify the projection onto the discrete constraint set. Then, given knowledge of memory layout and addressing schemes, an adversary can use, e.g., RowHammer [36], in order to flip as many of the adversarially selected bits. Note that, in practice, not all of these bits will be vulnerable to an end-to-end RowHammer attack on memory, which we do not focus on. However, from a robustness viewpoint, it makes sense to consider a slightly stronger threat model than actually realistic. Overall, our white-box threat model is defined as follows:

An adversary can flip up to $\epsilon := \lceil pmW \rceil$ bits, at most one bit per (quantized) weight value, in order to reduce accuracy and has full access to the DNN, its weights and gradients.

Following the projected gradient ascent approach of [28] and letting d_H be the (bit-level) Hamming distance, we intend to maximize cross-entropy loss \mathcal{L} on a mini-batch $\{(x_b, y_b)\}_{b=1}^B$ of examples:

$$\max_{\tilde{v}} \sum_{b=1}^B \mathcal{L}(f(x_b; Q^{-1}(\tilde{v})), y_b) \quad \text{s.t.} \quad d_H(\tilde{v}, v) \leq \epsilon, \quad d_H(\tilde{v}_i, v_i) \leq 1 \quad (2)$$

As made explicit in Eq. (2), we work on bit-level, i.e., optimize over the signed integer representation $\tilde{v}_i \in \{2^{m-1}, \dots, 2^{m-1} - 1\}$ corresponding to the underlying bits of the perturbed weights $\tilde{w} = Q(\tilde{v})$. We will adversarially inject bit errors based on the gradient of Eq. (2) and perform a projection onto the Hamming constraints $d_H(\tilde{v}, v) \leq \epsilon$ and $d_H(\tilde{v}_i, v_i) \leq 1$ with respect to the quantized, clean weights $v = Q(w)$. This means that we maximize Eq. (2) through projected gradient ascent where the forward and backward pass are performed in floating point:

$$\tilde{w}^{(t+1)} = \tilde{w}^{(t)} + \gamma \Delta^{(t)} \quad \text{with} \quad \Delta^{(t)} = \sum_{b=1}^B \nabla_w \mathcal{L}(f(x_b; \tilde{w}_q^{(t)}), y_b), \quad \tilde{w}_q^{(t)} = Q^{-1}(Q(\tilde{w}^{(t)})) \quad (3)$$

followed by the projection of $\tilde{v}^{(t+1)} = Q(\tilde{w}^{(t+1)})$ onto the (bit-level) Hamming constraints of Eq. (2). Here, γ is the step size. The updates are performed in floating point, while the forward pass is performed using the de-quantized weights $\tilde{w}_q^{(t)}$. The perturbed weights $\tilde{w}^{(0)} = Q^{-1}(\tilde{v}^{(0)})$ are initialized by uniformly picking $k \in [0, \epsilon]$ bits to be flipped in $v = Q(w)$ in order to obtain $\tilde{v}^{(0)}$. Overall, our adversarial bit attack is summarized in Alg. 1.

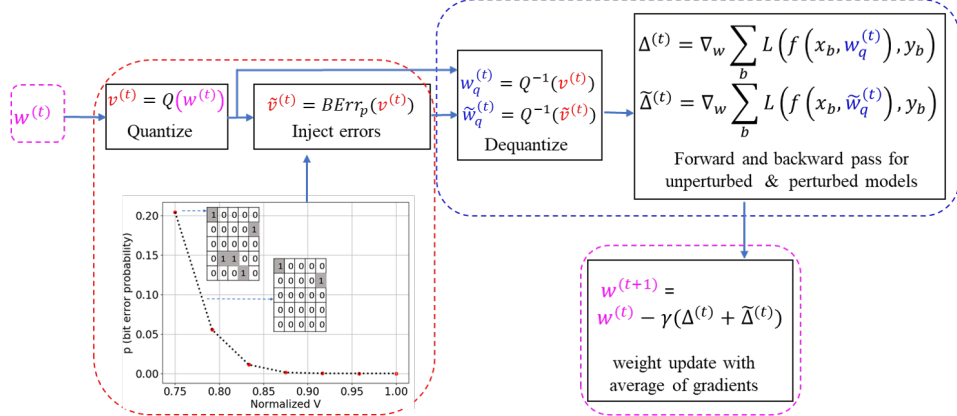


Figure 2: **Random Bit Error Training Illustration.** We illustrate the data-flow for *random bit error training* as in Alg. 1, when $\lambda = 1$. Here, BErr_p injects random bit errors in the *signed m -bit integers* $v^{(t)} = Q(w^{(t)})$, resulting in $\tilde{v}^{(t)}$, while the forward pass is performed on the *de-quantized perturbed weights* $\tilde{w}_q^{(t)} = Q^{-1}(\tilde{v}^{(t)})$, i.e., fixed-point arithmetic is not emulated. The weight update during training is not affected by bit errors and computed in *floating point*. Color coding follows Alg. 1.

The Hamming-projection is similar to the L_0 projection used for adversarial inputs, e.g., in [44]. Dropping the superscript t for brevity, in each iteration, we solve the following projection problem:

$$\min_{\tilde{v}'} \|Q^{-1}(\tilde{v}) - Q^{-1}(\tilde{v}')\|_2^2 \quad \text{s.t.} \quad d_H(v_i, \tilde{v}'_i) \leq 1, \quad d_H(v, \tilde{v}') \leq \epsilon \quad (4)$$

where $\tilde{v} = Q(\tilde{w})$ are the quantized, perturbed weights after Eq. (3), $\tilde{w}' = Q^{-1}(\tilde{v}')$ will be the perturbed weights after projection, and $v = Q(w)$ are the quantized, clean weights. This can be solved in two steps as the objective and the constraint set are separable: The first step involves keeping only the top- ϵ changed values, i.e., the top- ϵ weights with the largest difference $|w_i - \tilde{w}_i|$. The second step can be solved by keeping only the most significant bit changed in \tilde{v}_i compared to v_i .

The optimization problem in Eq. (2) is challenging due to the projection onto the non-convex set of Hamming constraints. We adopt best practices from computing adversarial inputs: normalizing the gradient [44] and backtracking [45]. Gradient normalization includes dividing by the L_1 norm $\|\Delta^{(t)}\|_1$, and then by the corresponding maximum absolute value. Using backtracking, the update in each iteration is only kept if the cross-entropy loss increases, otherwise, the step size γ is reduced. In spite of these optimization tricks, Alg. 1 remains very sensitive to hyper-parameters.

4 Robustness through Random and Adversarial Bit Error Training

We aim to obtain robustness against random and adversarial bit errors through *bit error training*. Robustness against random bit errors of probability p , caused by low-voltage operation, has to induce robustness for bit errors with lower probability $p' \leq p$, as well. In practice, this allows to operate accelerators over a wider range of voltages. Here, we aim to preserve the *average-case robust test error*, i.e., the test error under the influence of bit errors, and keep the standard deviation low in order to generalize to many different bit error patterns or spatial distribution of errors corresponding to different chips. Robustness to adversarial bit errors is measured in terms of *worst-case* robust test error that an adversary can obtain within a fixed budget of allowed bit flips, i.e., $\epsilon := \lceil pmW \rceil$. Additionally, robustness against random bit errors with significantly higher p is desirable to “defend” against malicious reductions in operating voltage.

Aggressive Clipping: As first step towards robustness, we aggressively reduce the quantization range w_{\max} . This is similar in spirit to learning quantization ranges [46, 38], but with robustness in mind. Smaller $w_{\max} > 0$ will increase resolution of the quantization, by reducing Δ in Eq. (1), while restricting the range of allowed weight values. Weight values are clipped to $[-w_{\max}, w_{\max}]$ which is then quantized with m bits, i.e., 2^m distinct values. Bit flips are injected post quantization such that reducing w_{\max} has the effect of restricting the range of perturbed weights, as well.

Random Bit Error Training (RANDBET): Injecting random bit errors with probability p during training results in the following learning problem, which we optimize as illustrated in Fig. 2:

$$\min_w \mathbb{E}[\mathcal{L}(f(x; \tilde{w}), y) + \lambda \mathcal{L}(f(x; w), y)] \quad \text{s.t.} \quad \tilde{w} = Q^{-1}(\tilde{v}), \tilde{v} = \text{BErr}_p(v), v = Q(w). \quad (5)$$

Random Bit Errors on MNIST				F-MNIST				NORMAL, $w_{\max}=0.1$: Confidence on MNIST
Training	w_{\max}	Err in%	avg RErr in %	w_{\max} ($p=1\%$)	Err in%	avg RErr in %	$p=0.1$ $p=1$	
NORMAL	1	0.36	89.92 89.98	1	5.37	91.04 90.85		
NORMAL	0.1	0.29	3.71 68.67	0.25	5.58	88.67 90.71		
NORMAL	0.05	0.29	1.30 22.37	0.2	6.26	81.33 90.17		
RANDBET	1	0.63	90.16 90.12	1	10.24	42.33 47.54		
RANDBET	0.1	0.31	0.45 0.62	0.25	7.26	9.63 11.67		
RANDBET	0.05	0.37	0.52 0.69	0.2	6.76	8.99 10.78		

Table 1: **Effect of Clipping on Robustness.** Clipping, i.e., lowering w_{\max} in Eq. (1), improves robustness against random bit errors and allows to train with large error rates, e.g., 2.5% on MNIST. Too aggressive clipping increases test error (red), cf. F-MNIST, and reduces confidences (right).

where $v = Q(w)$ denotes the quantized weights w which are to be learned. $\text{BER}_p(v)$ injects random bit errors with rate p in v and $\lambda = 1$ (fixed in all experiments) means that we also consider the loss on clean weights. This is desirable to avoid an increase in (clean) test error and stabilize training compared to $\lambda = 0$ which corresponds to training only on bit errors in the weights. We use stochastic gradient descent to optimize Eq. (5), by performing the gradient computation using the perturbed weights $\tilde{w} = Q^{-1}(\tilde{v})$, while applying the gradient update on the clean weights w . In spirit, this is similar to data augmentation, however, the perturbation is applied on the weights instead of the inputs. We found that introducing bit errors right from the start may prevent the DNN from converging. Thus, we start applying bit errors as soon as the (clean) cross-entropy loss reaches 1.75 or below.

Adversarial Bit Error Training (AdvBET): Training with adversarial bit errors follows the formulation of Eq. (5). However, instead of random bit errors, adversarial bit errors are used, resulting in a min-max formulation similar to [28]:

$$\min_w \mathbb{E}[\max_{\tilde{v}} \mathcal{L}(f(x; Q^{-1}(\tilde{v})), y) + \lambda \mathcal{L}(f(x; w), y)] \quad \text{s.t. } d_H(\tilde{v}, v) \leq \epsilon, d_H(\tilde{v}_i, v_i) \leq 1 \quad (6)$$

where the maximization problem, i.e., the attack, is constrained in the number of bits that may be changed by $\epsilon := \lceil pmW \rceil$. Details are provided in Alg. 1. In addition to not training on adversarial bit errors for a (clean) cross-entropy above 1.75, we clip gradients to $[-0.05, 0.05]$. This is required as the cross-entropy loss on adversarially perturbed weights \tilde{w} can easily be one or two magnitudes larger than on the clean weights. Similarly, we found smaller learning rates for training to be necessary. Finally, training is very sensitive to the hyper-parameters of the attack in Alg. 1, including the step size, gradient normalization and backtracking. This holds both for convergence during training as well as for the obtained robustness after training. To overcome these problems, and in contrast to common practice in adversarial training on adversarial inputs [28], we randomize the attack hyper-parameters during training. This has the advantage of added stochasticity regularizing training and not over-fitting to a particular attack, providing improved robustness at test time.

5 Experiments

We conduct experiments on MNIST [23], Fashion-MNIST (F-MNIST) [24] and CIFAR10 [25]. We use SimpleNet [47] as it provides comparable performance as, e.g., VGG [48], with limited number of weights: roughly 5.5M on CIFAR10 vs. 14M for VGG16. On MNIST and F-MNIST, we halve all channel widths, resulting in roughly 1M weights. Additionally, we use group normalization (GN) [49] instead of batch normalization (BN) [50], as we found BN to reduce robustness significantly. We use $m = 16$ bits for quantization (during training and for injecting bit errors).

We report (**clean**) **test error Err** (lower is better, \downarrow), corresponding to *clean* weights, and **robust test error RErr** (\downarrow), the test error on *perturbed* weights, on 9000 test examples. For random bit errors with rate p in %, we report *average* RErr and its standard deviation across 50 samples of random bit errors with rate p , simulating 50 different chips. **Random bit error training (RANDBET)** uses $\lambda = 1$ in Eq. (5) and a fixed error rate p (for evaluation, p might be different). In contrast to [15], we do *not* change p during training. For adversarial bit errors, we report *worst-case* RErr and run 14 attacks with varying step sizes/gradient normalization/backtracking, three random restarts each ($3 \cdot 14 = 42$ individual attacks) and up to $T = 100$ iterations, computed on 100 held-out test examples. In **adversarial bit error training (AdvBET)**, we use $T = 10$ iterations, randomize step size/gradient normalization/backtracking, consider both $\lambda = 0$ as well as $\lambda = 1$ and disable learnable scale/bias of group normalization.

Random Bit Errors on MNIST with $w_{\max} = 0.1$						
Training, p in %	Err in % \downarrow	Average RErr in % \downarrow , p for evaluation in %				
		$p=0.1$	$p=0.5$	$p=1$	$p=1.5$	$p=2.5$
NORMAL, $w_{\max} = 1$	0.36	89.96 ± 1.41	89.92 ± 1.49	89.98 ± 1.59	89.93 ± 1.17	90.21 ± 1.23
NORMAL	0.29	0.40 ± 0.04	3.71 ± 4.53	68.67 ± 14.6	88.74 ± 2.78	90.02 ± 1.08
RANDBET, $p=1.5$	0.30	0.33 ± 0.02	0.41 ± 0.04	0.52 ± 0.06	0.69 ± 0.14	1.77 ± 0.69
RANDBET, $p=2.5$	0.37	0.39 ± 0.02	0.45 ± 0.03	0.51 ± 0.04	0.59 ± 0.07	0.86 ± 0.14
ADVBET $_{\lambda=1}$, $p=0.01$	0.49	0.51 ± 0.01	0.55 ± 0.02	0.60 ± 0.03	0.65 ± 0.05	0.78 ± 0.06
Random Bit Errors on F-MNIST with $w_{\max} = 0.25$						
Training, p in %	Err in % \downarrow	Average RErr in % \downarrow , p for evaluation in %				
		$p=0.01$	$p=0.05$	$p=0.1$	$p=0.5$	$p=1$
NORMAL, $w_{\max} = 1$	5.37	14.87 ± 4.05	88.69 ± 2.31	90.69 ± 1.3	91.04 ± 1.62	90.85 ± 1.4
NORMAL	5.58	6.44 ± 0.14	8.24 ± 0.43	12.34 ± 1.88	88.67 ± 2.14	90.71 ± 1.54
RANDBET, $p=0.1$	5.57	6.03 ± 0.09	6.83 ± 0.17	7.73 ± 0.31	52.51 ± 8.49	88.46 ± 2.09
RANDBET, $p=0.5$	6.19	6.44 ± 0.05	6.84 ± 0.13	7.22 ± 0.17	9.57 ± 0.62	16.39 ± 2.32
ADVBET $_{\lambda=1}$, $p=0.005$	8.44	8.70 ± 0.08	9.09 ± 0.13	9.47 ± 0.17	12.84 ± 0.97	26.79 ± 5.4
Random Bit Errors on CIFAR10 with $w_{\max} = 0.15$						
Training, p in %	Err in % \downarrow	Average RErr in % \downarrow , p for evaluation in %				
		$p=0.01$	$p=0.05$	$p=0.1$	$p=0.5$	$p=1$
NORMAL, $w_{\max} = 1$	8.32	27.39 ± 3.67	90.86 ± 0.81	90.84 ± 0.69	90.93 ± 0.53	90.81 ± 0.53
NORMAL	8.13	8.87 ± 0.12	10.01 ± 0.19	11.32 ± 0.32	51.13 ± 7.91	88.99 ± 1.55
RANDBET, $p=0.5$	8.23	8.63 ± 0.06	9.16 ± 0.13	9.63 ± 0.17	13.17 ± 0.49	20.93 ± 1.53
RANDBET, $p=1$	8.89	9.27 ± 0.08	9.74 ± 0.13	10.17 ± 0.17	12.59 ± 0.38	16.08 ± 0.83
ADVBET $_{\lambda=1}$, $p=0.001$	10.11	10.72 ± 0.07	11.49 ± 0.12	12.27 ± 0.17	22.40 ± 2.03	60.32 ± 8.16

Table 2: **Random Bit Errors.** Clean test error Err and *average* robust test error RErr for 50 samples of random bit errors of rate p . For RErr, we also report the standard deviation (in gray). RANDBET, with $\lambda = 1$, allows to operate with higher bit error rates, i.e., at lower voltages: $p = 2.5\%$ on MNIST and $p = 0.1\%$ on F-MNIST/CIFAR10 are tolerable. ADVBET, although trained with significantly fewer adversarial bit errors, generalizes to more, but random bit errors.

We refer to our **supplementary material** for more details on our error models and additional experiments regarding clipping, baselines, batch normalization, and bit error training.

5.1 Evaluation on Random Bit Errors

Clipping: Tab. 1 shows the impact of aggressive clipping, i.e., reducing w_{\max} , on Err and RErr against random bit errors. Both on MNIST and F-MNIST, reducing w_{\max} clearly improves robustness: clipping at $w_{\max} = 0.05$ on MNIST yields 1.3% RErr against bit errors with probability $p = 0.1\%$. However, as shown on F-MNIST (in red), extreme clipping can increase test error: $w_{\max} = 0.2$ with 6.26% Err compared to 5.37% with $w_{\max} = 1$ (i.e., no aggressive clipping). Similarly, clipping can reduce predicted confidences as shown in Tab. 1 (right) for MNIST and $w_{\max} = 0.1$ where the confidences are limited to ~ 0.7 . Clipping is also essential for successfully training with bit errors, i.e., RANDBET, as shown on F-MNIST where training with $p = 1\%$ bit errors and without aggressive clipping, i.e., $w_{\max} = 1$, increases Err to 10.24%. We provide additional experiments on the influence of clipping (logit distribution, activations etc.) in the supplement. Overall, we chose $w_{\max} = 0.1$ on MNIST, 0.25 on F-MNIST and 0.15 on CIFAR10.

Baseline: To emulate a robust DNN for a specific chip *and* operating voltage, similar to [12, 15], the rate p and spatial distribution of bit errors is fixed for training *and* testing. A DNN trained with $p = 1\%$ on MNIST obtains 1.3% RErr when tested against the same bit errors. However, RErr increases to 86% for the same model during testing with lower rate $p = 0.1\%$. This is unintuitive as the bit errors at $p = 0.1\%$ constitute a subset of those at $p = 1\%$. Moreover, RErr increases to 90% on injecting random bit patterns during testing with $p = 1\%$. We suspect that DNNs treat fixed bit errors as “additive biases” and start to rely on them, see the supplement for more results. Thus, there is no generalization to other bit error patterns, i.e., other chips/memory arrays or operating voltages. Voltage, however, is usually controlled dynamically [13] and training a model for each operating voltage and chip is clearly infeasible.

Bit Error Training: Tab. 2 reports *average* RErr on random bit errors for different error rates p for training and evaluation. The shown bit error rates p for training (in blue) are chosen to keep Err close

Adversarial Bit Errors on MNIST, $w_{\max} = 0.1$				F-MNIST, $w_{\max} = 0.25$				CIFAR10, $w_{\max} = 0.15$				
Training, p in %	Err in %	Worst RErr in % ↓		Err in %	Worst RErr in % ↓		Err in %	Worst RErr in % ↓		0.0005 0.001 0.005		
NORMAL	0.29	91.07	91.07	91.09	5.58	91.66	91.66	91.66	8.13	90.90	90.90	90.90
RANDBET, $p=1$	0.31	91.07	91.07	94.13	7.26	90.90	91.20	91.20	8.89	90.94	90.94	90.94
ADVBET $_{\lambda=1}$, P	0.49	10.54	21.43	89.86	8.44	18.06	29.86	91.33	10.11	20.68	63.04	90.36
ADVBET $_{\lambda=0}$, P	0.52	10.78	11.10	89.90	12.70	25.98	37.36	91.21	10.70	15.02	40.27	90.36

Table 3: **Adversarial Bit Errors.** *Worst-case* robust test error RErr across 14 adversarial bit attacks each with 3 restarts per model and rate p , with up to 100 iterations and varying step sizes. NORMAL and RANDBET ($p = 1\%$ and $\lambda = 1$) are not robust against adversarial bit flips. ADVBET, trained on adversarial bit error rate p marked in **blue** proves effective against adversarial bit attacks with same or lower rate, however, does not generalize to significantly larger rates (in **red**).

to normal training. On F-MNIST, for example, $p = 0.1\%$ results in 5.57% Err compared to 5.37% for the normal model, while $p = 0.5\%$ further increases Err to 6.19%. Regarding evaluation with random bit errors, RANDBET allows robust operation for a bit error rate up to $p = 2.5\%$ on MNIST: 0.86% RErr compared to 90% for normal training, even with clipping. In Fig. 1, this corresponds to a reduction in energy consumption per SRAM access of more than 30%. On F-MNIST and CIFAR10, RErr increases faster with bit error rate p : $p = 0.1\%$ can be tolerated with 7.22% RErr and 9.63% RErr, respectively. This still results in energy savings of more than 22%. In all cases, standard deviation (in gray) is below 0.2% and RErr monotonically decreases with lower p , indicating that our models generalize to different chips/memory arrays and higher supply voltages. Surprisingly, ADVBET generalizes to random bit errors with significantly larger rate p than seen during training.

Results with Batch Normalization (BN): We found that DNNs with BN are more vulnerable to bit errors. For SimpleNet on MNIST, RErr for RANDBET trained and tested at $p = 1.5\%$ increases from 0.69% to 9.74% when using BN. The discrepancy increases on F-MNIST/CIFAR10 and when considering ResNets [51], which are particularly dependent on BN [52], see the supplement. Similarly, adversarial bit error training was not effective with BN. This is supported by [22] where training ResNets on adversarial bit errors does *not* improve robustness. We suspect that the batch normalization statistics play a key role, as in adversarial training on adversarial inputs [53].

5.2 Evaluation on Adversarial Bit Errors

Tab. 3 reports *worst-case* RErr against adversarial bit errors. Few adversarial bit flips are sufficient to obtain high RErr for NORMAL and RANDBET: $p = 0.0005\%$ corresponding to $\epsilon := \lceil pmW \rceil = 440$ on CIFAR10 and $p = 0.005\%$ corresponding to $\epsilon = 864$ on MNIST/F-MNIST. We note that different from adversarial inputs, our adversarial bit attack cannot degrade RErr to 100%. Instead, our attack is successful when the DNN generates random output, i.e., $\sim 90\%$ RErr. Our ADVBET provides low RErr for p equal or lower than used during training (in **blue**): for example, 11.1% on MNIST and 29.86% on F-MNIST. Except on F-MNIST, $\lambda = 0$ results in better robustness, while increasing Err compared to $\lambda = 1$. However, as with training on adversarial inputs [45], robustness does not generalize to higher p than seen during training (in **red**). While hard to compare, [22] reports that 541 bits of their (robust) binarized ResNet-20 need to be flipped for $\sim 90\%$ RErr, while we obtain 40.27% for up to $\epsilon = 879$ bit errors. As shown in Tab. 2, ADVBET $_{\lambda=1}$ also improves robustness against a higher percentage of *random* bit errors as, e.g., caused by adversarial voltage reduction.

6 Conclusion

We studied random and adversarial bit errors on (quantized) DNN weights. Random bit errors occur in SRAM and DRAM of DNN accelerators when operating with low voltage in order to save energy, e.g., [13, 15, 12]. Additionally, random bit errors can be provoked by an adversary maliciously reducing voltage. Adversarial bit errors have been shown realistic in recent work [36, 9, 8] and, thus, pose a severe security threat. We made first steps towards training DNNs robust to random and adversarial bit errors, by explicitly taking such errors into account during training. We obtain DNNs robust to random bit errors, allowing low-voltage operation at multiple operating voltages and across many chips with their unique bit error patterns. Furthermore, we can reduce the worst-case test error under adversarial bit attacks significantly, while additionally providing robustness to random bit errors from maliciously reduced voltage.

Broader Impact

On the positive side, this paper aims at increasing robustness of deep neural networks (DNNs) which we consider as an important goal to ensure positive impact of machine learning on our society. In particular, robustness against bit errors, as discussed in this paper, has the potential to lead to improved energy-efficiency of DNN accelerators due to low-voltage operation. Obviously, improved energy-efficiency while maintaining the same prediction performance is a desirable goal.

On the negative side as we are discussing defenses against adversarial manipulation of the DNN weights on a bit-level we also have to discuss attacks to challenge the defense. Thus, we introduce and discuss bit-level adversarial attacks on the weights which, in principle, could be abused to attack an “undefended” model. However, this kind of conflict is unavoidable when discussing security relevant issues of machine learning systems.

References

- [1] Yu-Hsin Chen, Joel S. Emer, and Vivienne Sze. Eyeriss: A spatial architecture for energy-efficient dataflow for convolutional neural networks. In *ACM/IEEE Annual International Symposium on Computer Architecture (ISCA)*, 2016.
- [2] Tianshi Chen, Zidong Du, Ninghui Sun, Jia Wang, Chengyong Wu, Yunji Chen, and Olivier Temam. Diannao: a small-footprint high-throughput accelerator for ubiquitous machine-learning. In *Architectural Support for Programming Languages and Operating Systems (ASPLOS)*, 2014.
- [3] Zidong Du, Robert Fasthuber, Tianshi Chen, Paolo Inen, Ling Li, Tao Luo, Xiaobing Feng, Yunji Chen, and Olivier Temam. Shidiannao: shifting vision processing closer to the sensor. In *ACM/IEEE Annual International Symposium on Computer Architecture (ISCA)*, 2015.
- [4] Hardik Sharma, Jongse Park, Naveen Suda, Liangzhen Lai, Benson Chau, Joon Kyung Kim, Vikas Chandra, and Hadi Esmaeilzadeh. Bit fusion: Bit-level dynamically composable architecture for accelerating deep neural networks. In *ACM/IEEE Annual International Symposium on Computer Architecture (ISCA)*, 2018.
- [5] NVIDIA Deep Learning Accelerator. <http://nvdla.org/>.
- [6] Shrikanth Ganapathy, John Kalamatianos, Keith Kasprak, and Steven Raasch. On characterizing near-threshold SRAM failures in FinFET technology. In *Proc. of the ACM Annual Design Automation Conference (DAC)*, 2017.
- [7] Zheng Guo, Andrew Carlson, Liang-Teck Pang, Kenneth Duong, Tsu-Jae King Liu, and Borivoje Nikolic. Large-scale SRAM variability characterization in 45 nm CMOS. *IEEE Journal of Solid-State Circuits*, 44(11), 2009.
- [8] Adrian Tang, Simha Sethumadhavan, and Salvatore J. Stolfo. CLKSCREW: exposing the perils of security-oblivious energy management. In *USENIX Security Symposium*, 2017.
- [9] Kit Murdock, David Oswald, Flavio D. Garcia, Jo Van Bulck, Daniel Gruss, and Frank Piessens. Plunder-volt: Software-based fault injection attacks against intel sgx. In *Proc. of the IEEE Symposium on Security and Privacy (SP)*, 2020.
- [10] Adnan Siraj Rakin, Zhezhi He, and Deliang Fan. Bit-flip attack: Crushing neural network with progressive bit search. In *Proc. of the IEEE International Conference on Computer Vision (ICCV)*, 2019.
- [11] Shrikanth Ganapathy, John Kalamatianos, Bradford M. Beckmann, Steven Raasch, and Lukasz G. Szafaryn. Killi: Runtime fault classification to deploy low voltage caches without MBIST. In *IEEE International Symposium on High Performance Computer Architecture (HPCA)*, 2019.
- [12] Sung Kim, Patrick Howe, Thierry Moreau, Armin Alaghi, Luis Ceze, and Visvesh Sathe. MATIC: learning around errors for efficient low-voltage neural network accelerators. In *Proc. of the Design, Automation & Test in Europe Conference & Exhibition (DATE)*, 2018.
- [13] Nandhini Chandramoorthy, Karthik Swaminathan, Martin Cochet, Arun Paidimari, Schuyler Eldridge, Rajiv V. Joshi, Matthew M. Ziegler, Alper Buyuktosunoglu, and Pradip Bose. Resilient low voltage accelerators for high energy efficiency. In *IEEE International Symposium on High Performance Computer Architecture (HPCA)*, 2019.
- [14] Brandon Reagen, Paul N. Whatmough, Robert Adolf, Saketh Rama, Hyunkwang Lee, Sae Kyu Lee, José Miguel Hernández-Lobato, Gu-Yeon Wei, and David M. Brooks. Minerva: Enabling low-power, highly-accurate deep neural network accelerators. In *ACM/IEEE Annual International Symposium on Computer Architecture (ISCA)*, 2016.

[15] Skanda Koppula, Lois Orosa, Abdullah Giray Yaglikçi, Roknoddin Azizi, Taha Shahroodi, Konstantinos Kanellopoulos, and Onur Mutlu. EDEN: enabling energy-efficient, high-performance deep neural network inference using approximate DRAM. In *Proc. of the Annual IEEE/ACM International Symposium on Microarchitecture*, 2019.

[16] Nicholas Cheney, Martin Schrimpf, and Gabriel Kreiman. On the robustness of convolutional neural networks to internal architecture and weight perturbations. *arXiv.org*, abs/1703.08245, 2017.

[17] Abhishek Murthy, Himel Das, and Md. Ariful Islam. Robustness of neural networks to parameter quantization. *arXiv.org*, abs/1903.10672, 2019.

[18] Paul Merolla, Rathinakumar Appuswamy, John V. Arthur, Steven K. Esser, and Dharmendra S. Modha. Deep neural networks are robust to weight binarization and other non-linear distortions. *arXiv.org*, abs/1606.01981, 2016.

[19] Wonyong Sung, Sungho Shin, and Kyuyeon Hwang. Resiliency of deep neural networks under quantization. *arXiv.org*, abs/1511.06488, 2015.

[20] Milad Alizadeh, Arash Behboodi, Mart van Baalen, Christos Louizos, Tijmen Blankevoort, and Max Welling. Gradient ℓ_1 regularization for quantization robustness. In *Proc. of the International Conference on Learning Representations (ICLR)*, 2020.

[21] Tsui-Wei Weng, Pu Zhao, Sijia Liu, Pin-Yu Chen, Xue Lin, and Luca Daniel. Towards certificated model robustness against weight perturbations. In *Proc. of the Conference on Artificial Intelligence (AAAI) Workshops*, 2020.

[22] Zhezhi He and Adnan Siraj Rakin, Jingtao Li, Chaitali Chakrabarti, and Deliang Fan. Defending and harnessing the bit-flip based adversarial weight attack. In *Proc. of the IEEE Conference on Computer Vision and Pattern Recognition (CVPR)*, 2020.

[23] Yann LeCun, Léon Bottou, Yoshua Bengio, and Patrick Haffner. Gradient-based learning applied to document recognition. *Proc. of the IEEE*, 86(11), 1998.

[24] Han Xiao, Kashif Rasul, and Roland Vollgraf. Fashion-MNIST: a novel image dataset for benchmarking machine learning algorithms. *arXiv.org*, abs/1708.07747, 2017.

[25] Alex Krizhevsky. Learning multiple layers of features from tiny images. Technical report, 2009.

[26] Chalapathy Neti, Michael H. Schneider, and Eric D. Young. Maximally fault tolerant neural networks. *IEEE Trans. on Neural Networks (TNN)*, 3(1), 1992.

[27] Ching-Tai Chiu, Kishan Mehrotra, Chilukuri K. Mohan, and Sanjay Ranka. Training techniques to obtain fault-tolerant neural networks. In *Annual International Symposium on Fault-Tolerant Computing*, 1994.

[28] Aleksander Madry, Aleksandar Makelov, Ludwig Schmidt, Dimitris Tsipras, and Adrian Vladu. Towards deep learning models resistant to adversarial attacks. *Proc. of the International Conference on Learning Representations (ICLR)*, 2018.

[29] Yujie Ji, Xinyang Zhang, Shouling Ji, Xiapu Luo, and Ting Wang. Model reuse attacks on deep learning systems. In *Proc. of the ACM Conference on Computer and Communications Security*, 2018.

[30] Jacob Dumford and Walter J. Scheirer. Backdooring convolutional neural networks via targeted weight perturbations. *arXiv.org*, abs/1812.03128, 2018.

[31] Sungho Shin, Yoonho Boo, and Wonyong Sung. Fixed-point optimization of deep neural networks with adaptive step size retraining. In *Proc. of the IEEE Conference on Acoustics, Speech and Signal Processing (ICASSP)*, 2017.

[32] Darryl Dexu Lin, Sachin S. Talathi, and V. Sreekanth Annapureddy. Fixed point quantization of deep convolutional networks. In *Proc. of the International Conference on Machine Learning (ICML)*, 2016.

[33] Hao Li, Soham De, Zheng Xu, Christoph Studer, Hanan Samet, and Tom Goldstein. Training quantized nets: A deeper understanding. In *Advances in Neural Information Processing Systems (NeurIPS)*, 2017.

[34] Kevin K. Chang, Abdullah Giray Yaalikçi, Saugata Ghose, Aditya Agrawal, Niladri Chatterjee, Abhijith Kashyap, Donghyuk Lee, Mike O’Connor, Hasan Hassan, and Onur Mutlu. Understanding reduced-voltage operation in modern DRAM devices: Experimental characterization, analysis, and mechanisms. *Proc. of the ACM on Measurement and Analysis of Computing Systems*, 1(1), 2017.

[35] Gopalakrishnan Srinivasan, Parami Wijesinghe, Syed Shakib Sarwar, Akhilesh Jaiswal, and Kaushik Roy. Significance driven hybrid 8t-6t SRAM for energy-efficient synaptic storage in artificial neural networks. In *Proc. of the Design, Automation & Test in Europe Conference & Exhibition (DATE)*, 2016.

[36] Yoongu Kim, Ross Daly, Jeremie Kim, Chris Fallin, Ji-Hye Lee, Donghyuk Lee, Chris Wilkerson, Konrad Lai, and Onur Mutlu. Flipping bits in memory without accessing them: An experimental study of DRAM disturbance errors. In *ACM/IEEE Annual International Symposium on Computer Architecture (ISCA)*, 2014.

[37] Mohammad Rastegari, Vicente Ordonez, Joseph Redmon, and Ali Farhadi. Xnor-net: Imagenet classification using binary convolutional neural networks. In *Proc. of the European Conference on Computer Vision (ECCV)*, 2016.

[38] Jungwook Choi, Zhuo Wang, Swagath Venkataramani, Pierce I-Jen Chuang, Vijayalakshmi Srinivasan, and Kailash Gopalakrishnan. PACT: parameterized clipping activation for quantized neural networks. *arXiv.org*, abs/1805.06085, 2018.

[39] Itay Hubara, Matthieu Courbariaux, Daniel Soudry, Ran El-Yaniv, and Yoshua Bengio. Quantized neural networks: Training neural networks with low precision weights and activations. *Journal of Machine Learning Research (JMLR)*, 18, 2017.

[40] Frank Seide, Hao Fu, Jasha Droppo, Gang Li, and Dong Yu. 1-bit stochastic gradient descent and its application to data-parallel distributed training of speech dnns. In *Annual Conference of the International Speech Communication Association*, 2014.

[41] Dan Alistarh, Demjan Grubic, Jerry Li, Ryota Tomioka, and Milan Vojnovic. QSGD: communication-efficient SGD via gradient quantization and encoding. In *Advances in Neural Information Processing Systems (NeurIPS)*, 2017.

[42] Shuchang Zhou, Zekun Ni, Xinyu Zhou, He Wen, Yuxin Wu, and Yuheng Zou. Dorefa-net: Training low bitwidth convolutional neural networks with low bitwidth gradients. *arXiv.org*, abs/1606.06160, 2016.

[43] Jakub Breier, Xiaolu Hou, Dirmanto Jap, Lei Ma, Shivam Bhasin, and Yang Liu. Practical fault attack on deep neural networks. In *Proc. of the ACM Conference on Computer and Communications Security*, 2018.

[44] Francesco Croce and Matthias Hein. Sparse and imperceptible adversarial attacks. In *Proc. of the IEEE International Conference on Computer Vision (ICCV)*, 2019.

[45] David Stutz, Matthias Hein, and Bernt Schiele. Confidence-calibrated adversarial training: Generalizing to unseen attacks. *Proc. of the International Conference on Machine Learning (ICML)*, 2020.

[46] Kuan Wang, Zhijian Liu, Yujun Lin, Ji Lin, and Song Han. HAQ: hardware-aware automated quantization with mixed precision. In *Proc. of the IEEE Conference on Computer Vision and Pattern Recognition (CVPR)*, 2019.

[47] Seyyed Hosseini HasanPour, Mohammad Rouhani, Mohsen Fayyaz, and Mohammad Sabokrou. Lets keep it simple, using simple architectures to outperform deeper and more complex architectures. *arXiv.org*, abs/1608.06037, 2016.

[48] Karen Simonyan and Andrew Zisserman. Very deep convolutional networks for large-scale image recognition. In *Proc. of the International Conference on Learning Representations (ICLR)*, 2015.

[49] Yuxin Wu and Kaiming He. Group normalization. In *Proc. of the European Conference on Computer Vision (ECCV)*, 2018.

[50] Sergey Ioffe and Christian Szegedy. Batch normalization: Accelerating deep network training by reducing internal covariate shift. In *Proc. of the International Conference on Machine Learning (ICML)*, 2015.

[51] Kaiming He, Xiangyu Zhang, Shaoqing Ren, and Jian Sun. Deep residual learning for image recognition. In *Proc. of the IEEE Conference on Computer Vision and Pattern Recognition (CVPR)*, 2016.

[52] Hongyi Zhang, Yann N. Dauphin, and Tengyu Ma. Fixup initialization: Residual learning without normalization. In *Proc. of the International Conference on Learning Representations (ICLR)*, 2019.

[53] Cihang Xie, Mingxing Tan, Boqing Gong, Jiang Wang, Alan L. Yuille, and Quoc V. Le. Adversarial examples improve image recognition. *arXiv.org*, abs/1911.09665, 2019.

[54] Battista Biggio and Fabio Roli. Wild patterns: Ten years after the rise of adversarial machine learning. *arXiv.org*, abs/1712.03141, 2018.

[55] Han Xu, Yao Ma, Haochen Liu, Debayan Deb, Hui Liu, Jiliang Tang, and Anil K. Jain. Adversarial attacks and defenses in images, graphs and text: A review. *arXiv.org*, abs/1909.08072, 2019.

[56] Christian Szegedy, Wojciech Zaremba, Ilya Sutskever, Joan Bruna, Dumitru Erhan, Ian Goodfellow, and Rob Fergus. Intriguing properties of neural networks. *arXiv.org*, abs/1312.6199, 2013.

[57] Nicholas Carlini and David Wagner. Towards evaluating the robustness of neural networks. In *Proc. of the IEEE Symposium on Security and Privacy (SP)*, 2017.

[58] Yinpeng Dong, Fangzhou Liao, Tianyu Pang, Xiaolin Hu, and Jun Zhu. Boosting adversarial attacks with momentum. *arXiv.org*, abs/1710.06081, 2017.

[59] Ping-Yeh Chiang, Jonas Geiping, Micah Goldblum, Tom Goldstein, Renkun Ni, Steven Reich, and Ali Shafahi. Witchcraft: Efficient PGD attacks with random step size. *arXiv.org*, abs/1911.07989, 2019.

[60] Francesco Croce and Matthias Hein. Reliable evaluation of adversarial robustness with an ensemble of diverse parameter-free attacks. *arXiv.org*, abs/2003.01690, 2020.

[61] Pin-Yu Chen, Huan Zhang, Yash Sharma, Jinfeng Yi, and Cho-Jui Hsieh. ZOO: Zeroth order optimization based black-box attacks to deep neural networks without training substitute models. In *Proc. of the ACM Workshop on Artificial Intelligence and Security*, 2017.

[62] Andrew Ilyas, Logan Engstrom, Anish Athalye, and Jessy Lin. Black-box adversarial attacks with limited queries and information. In *Proc. of the International Conference on Machine Learning (ICML)*, 2018.

[63] Francesco Croce and Matthias Hein. Sparse and imperceptible adversarial attacks. *arXiv.org*, abs/1909.05040, 2019.

[64] Maksym Andriushchenko, Francesco Croce, Nicolas Flammarion, and Matthias Hein. Square attack: a query-efficient black-box adversarial attack via random search. *arXiv.org*, abs/1912.00049, 2019.

[65] Yanpei Liu, Xinyun Chen, Chang Liu, and Dawn Song. Delving into transferable adversarial examples and black-box attacks. *arXiv.org*, abs/1611.02770, 2016.

[66] Jiajun Lu, Hussein Sibai, Evan Fabry, and David Forsyth. No need to worry about adversarial examples in object detection in autonomous vehicles. *arXiv.org*, abs/1707.03501, 2017.

[67] Alexey Kurakin, Ian Goodfellow, and Samy Bengio. Adversarial examples in the physical world. *arXiv.org*, abs/1607.02533, 2016.

[68] Jonathan Peck, Joris Roels, Bart Goossens, and Yvan Saeys. Lower bounds on the robustness to adversarial perturbations. In *Advances in Neural Information Processing Systems (NeurIPS)*, 2017.

[69] Huan Zhang, Tsui-Wei Weng, Pin-Yu Chen, Cho-Jui Hsieh, and Luca Daniel. Efficient neural network robustness certification with general activation functions. In *Advances in Neural Information Processing Systems (NeurIPS)*, 2018.

[70] Eric Wong and J. Zico Kolter. Provable defenses against adversarial examples via the convex outer adversarial polytope. In *Proc. of the International Conference on Machine Learning (ICML)*, 2018.

[71] Sven Gowal, Krishnamurthy Dvijotham, Robert Stanforth, Rudy Bunel, Chongli Qin, Jonathan Uesato, Relja Arandjelovic, Timothy A. Mann, and Pushmeet Kohli. On the effectiveness of interval bound propagation for training verifiably robust models. *arXiv.org*, abs/1810.12715, 2018.

[72] Takeru Miyato, Shin-ichi Maeda, Masanori Koyama, Ken Nakae, and Shin Ishii. Distributional smoothing with virtual adversarial training. *arXiv.org*, abs/1507.00677, 2015.

[73] Ruitong Huang, Bing Xu, Dale Schuurmans, and Csaba Szepesvári. Learning with a strong adversary. *arXiv.org*, abs/1511.03034, 2015.

[74] David Stutz, Matthias Hein, and Bernt Schiele. Disentangling adversarial robustness and generalization. *Proc. of the IEEE Conference on Computer Vision and Pattern Recognition (CVPR)*, 2019.

[75] Dimitris Tsipras, Shibani Santurkar, Logan Engstrom, Alexander Turner, and Aleksander Madry. Robustness may be at odds with accuracy. *arXiv.org*, abs/1805.12152, 2018.

[76] Yair Carmon, Aditi Raghunathan, Ludwig Schmidt, Percy Liang, and John C. Duchi. Unlabeled data improves adversarial robustness. *arXiv.org*, abs/1905.13736, 2019.

[77] Jonathan Uesato, Jean-Baptiste Alayrac, Po-Sen Huang, Robert Stanforth, Alhussein Fawzi, and Pushmeet Kohli. Are labels required for improving adversarial robustness? *arXiv.org*, abs/1905.13725, 2019.

[78] Florian Tramèr and Dan Boneh. Adversarial training and robustness for multiple perturbations. *arXiv.org*, abs/1904.13000, 2019.

[79] Pratyush Maini, Eric Wong, and J. Zico Kolter. Adversarial robustness against the union of multiple perturbation models. *arXiv.org*, abs/1909.04068, 2019.

[80] Elias B. Khalil, Amrita Gupta, and Bistra Dilkina. Combinatorial attacks on binarized neural networks. In *Proc. of the International Conference on Learning Representations (ICLR)*, 2019.

[81] Norman Mu and Justing Gilmer. Mnist-c: A robustness benchmark for computer vision. *Proc. of the International Conference on Machine Learning (ICML) Workshops*, 2019.

[82] Dan Hendrycks and Thomas G. Dietterich. Benchmarking neural network robustness to common corruptions and perturbations. *arXiv.org*, abs/1903.12261, 2019.

[83] Raphael Gontijo Lopes, Dong Yin, Ben Poole, Justin Gilmer, and Ekin D Cubuk. Improving robustness without sacrificing accuracy with patch gaussian augmentation. In *Proc. of the International Conference on Machine Learning (ICML) Workshops*, 2019.

[84] Daniel Kang, Yi Sun, Dan Hendrycks, Tom Brown, and Jacob Steinhardt. Testing robustness against unforeseen adversaries. *arXiv.org*, abs/1908.08016, 2019.

[85] Dipti Deodhare, M. Vidyasagar, and S. Sathiya Keerthi. Synthesis of fault-tolerant feedforward neural networks using minimax optimization. *IEEE Trans. on Neural Networks (TNN)*, 9(5), 1998.

- [86] Faiz Ur Rahman, Bhavan Vasu, and Andreas E. Savakis. Resilience and self-healing of deep convolutional object detectors. In *Proc. of the IEEE International Conference on Image Processing (ICIP)*, 2018.
- [87] Vasisht Duddu, D. Vijay Rao, and Valentina E. Balas. Adversarial fault tolerant training for deep neural networks. *arXiv.org*, abs/1907.03103, 2019.
- [88] Vasisht Duddu, N. Rajesh Pillai, D. Vijay Rao, and Valentina E. Balas. Fault tolerance of neural networks in adversarial settings. *arXiv.org*, abs/1910.13875, 2019.
- [89] César Torres-Huitzil and Bernard Girau. Fault and error tolerance in neural networks: A review. *IEEE Access*, 5, 2017.
- [90] Yingqi Liu, Shiqing Ma, Yousra Aafer, Wen-Chuan Lee, Juan Zhai, Weihang Wang, and Xiangyu Zhang. Trojaning attack on neural networks. In *Annual Network and Distributed System Security Symposium*, 2018.
- [91] Cong Liao, Haoti Zhong, Anna Cinzia Squicciarini, Sencun Zhu, and David J. Miller. Backdoor embedding in convolutional neural network models via invisible perturbation. *arXiv.org*, abs/1808.10307, 2018.
- [92] Jialong Zhang, Zhongshu Gu, Jiyong Jang, Hui Wu, Marc Ph. Stoecklin, Heqing Huang, and Ian Molloy. Protecting intellectual property of deep neural networks with watermarking. In *Proc. of the ACM on Asia Conference on Computer and Communications Security (AsiaCCS)*, 2018.
- [93] Andrew G. Howard, Menglong Zhu, Bo Chen, Dmitry Kalenichenko, Weijun Wang, Tobias Weyand, Marco Andreetto, and Hartwig Adam. Mobilenets: Efficient convolutional neural networks for mobile vision applications. *arXiv.org*, abs/1704.04861, 2017.
- [94] Xiangyu Zhang, Xinyu Zhou, Mengxiao Lin, and Jian Sun. Shufflenet: An extremely efficient convolutional neural network for mobile devices. In *Proc. of the IEEE Conference on Computer Vision and Pattern Recognition (CVPR)*, 2018.
- [95] Forrest N. Iandola, Matthew W. Moskewicz, Khalid Ashraf, Song Han, William J. Dally, and Kurt Keutzer. SqueezeNet: Alexnet-level accuracy with 50x fewer parameters and <1mb model size. *arXiv.org*, abs/1602.07360, 2016.
- [96] Song Han, Huizi Mao, and William J. Dally. Deep compression: Compressing deep neural network with pruning, trained quantization and huffman coding. In *Proc. of the International Conference on Learning Representations (ICLR)*, 2016.
- [97] Jian-Hao Luo, Jianxin Wu, and Weiyao Lin. Thinet: A filter level pruning method for deep neural network compression. In *Proc. of the IEEE International Conference on Computer Vision (ICCV)*, 2017.
- [98] Yunhui Guo. A survey on methods and theories of quantized neural networks. *arXiv.org*, abs/1808.04752, 2018.
- [99] Raghuraman Krishnamoorthi. Quantizing deep convolutional networks for efficient inference: A whitepaper. *arXiv.org*, abs/1806.08342, 2018.
- [100] Matthieu Courbariaux, Yoshua Bengio, and Jean-Pierre David. Binaryconnect: Training deep neural networks with binary weights during propagations. In *Advances in Neural Information Processing Systems (NeurIPS)*, 2015.
- [101] Dan Alistarh, Jerry Li, Ryota Tomioka, and Milan Vojnovic. QSGD: randomized quantization for communication-optimal stochastic gradient descent. *arXiv.org*, abs/1610.02132, 2016.
- [102] Kaiming He, Xiangyu Zhang, Shaoqing Ren, and Jian Sun. Delving deep into rectifiers: Surpassing human-level performance on imagenet classification. In *Proc. of the IEEE International Conference on Computer Vision (ICCV)*, 2015.
- [103] Adam Paszke, Sam Gross, Soumith Chintala, Gregory Chanan, Edward Yang, Zachary DeVito, Zeming Lin, Alban Desmaison, Luca Antiga, and Adam Lerer. Automatic differentiation in pytorch. In *Advances in Neural Information Processing Systems (NeurIPS) Workshops*, 2017.

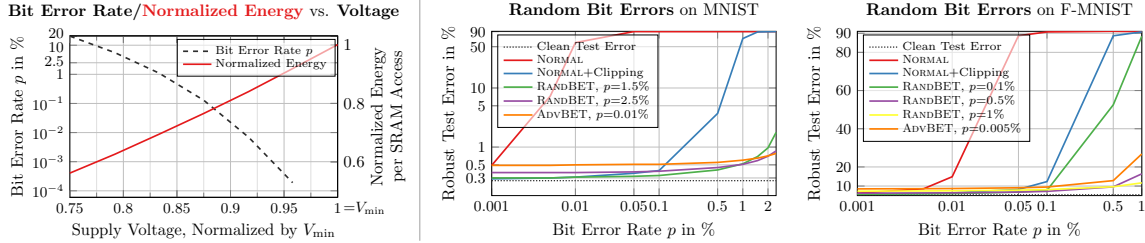


Figure 3: **Impact and Energy Savings of Random Bit Errors.** *Left:* Bit error rate and normalized energy per SRAM access plotted against supply voltage. Details on these measurements covered in Sec. B. *Middle and Right:* Robust test error, i.e., test error on quantized weights *with* bit errors, against bit error rate p in % on MNIST and F-MNIST. Normal training, even with clipping to $[-0.1, 0.1]$ on MNIST and $[-0.25, 0.25]$ on F-MNIST, exhibits severe accuracy drops starting with $p = 0.1\%$. Our random bit error training (RANDBET) results in significantly more robust DNNs.

A Overview

In the main paper, we studied the impact of random and adversarial bit errors on quantized deep neural network (DNN) weights. Random bit errors occur when optimizing DNN accelerators for energy efficiency [6, 11, 12, 13], while adversarial bit errors are motivated through recent attacks on accelerator memory [8, 9]. As first steps towards obtaining robust DNNs, we proposed **random bit error training (RANDBET)** and **adversarial bit error training (AdvBET)** leading to more robust DNNs and potentially improving energy-efficiency and security of DNN accelerators. This document provides further details on our random and adversarial bit error models and includes additional results regarding clipping, batch normalization, baselines, and our bit error training.

Outline: In Sec. B, we discuss our introductory figure from the main paper in more detail, i.e., regarding the measurements for SRAM energy consumption. After a discussion of related work in the broad areas of adversarial robustness, fault tolerance, backdooring and quantization, we discuss our random and adversarial bit error models in more depth, cf. Sec. D.2 and Sec. D.3, respectively. Finally, Sec. E contains additional details on the experimental setup, in Sec. E.1, and further experiments: Results regarding clipping in Sec. E.2, a discussion of batch normalization in Sec. E.3, more results on random bit errors in Sec. E.4 and adversarial bit errors in Sec. E.5.

B Energy Savings in Figure 1

Fig. 3, corresponding to Fig. 1 of the main paper, shows bit error rate characterization results of SRAMs in the DNN accelerator chip described in [13], fabricated using 14nm FinFET technology. The average bit error rate is measured from 32 SRAMs, each SRAM array of size 4KB (512×64 bit), as supply voltage is scaled down. *Bit error rate p (in %)* at a given supply voltage is measured as the count of read or write bit cell failures averaged over the total number of bit cells in the SRAM. A bit cell failure refers to reading 1 on writing 0 or reading 0 on writing 1. For a more comprehensive characterisation of SRAMs in 14nm technology, the reader is referred to [6]. Fig. 3 also shows the energy per write and read access of a 4KB (512×64 bit) SRAM, obtained from Cadence Spectre simulations. Energy is obtained at the same constant clock frequency at all supply voltages. The voltage (x-axis) shown is normalized over V_{min} which is the lowest measured voltage at which there are no bit cell failures. Energy shown in the graph (secondary axis on the right) is also normalized over the energy per access at V_{min} .

Accelerators such as [1, 2, 13, 14, 5, 3, 4] have a large amount of on-chip SRAM to store weights and intermediate computations. Total dynamic energy of accelerator SRAMs can be obtained as the total number of SRAM accesses \times energy of a single SRAM access. Optimized dataflow in accelerators leads to better re-use of weights read from memories in computation, reducing the number of such memory accesses [1, 2, 5]. Low voltage operation focuses on reducing the memory access energy, leading to significant energy savings as shown.

C Related Work

In the following, we briefly review work on adversarial robustness, fault tolerance, backdooring and quantization. These areas are broadly related to the topic of the main paper.

Adversarial and Corruption Robustness: Robustness of DNNs against adversarially perturbed or randomly corrupted inputs received considerable attention in recent years, see, e.g., relevant surveys [54, 55]. Adversarial examples [56], i.e., nearly imperceptibly perturbed inputs causing misclassification, consider an adversarial environment where potential attackers can actively manipulate inputs. This has been shown to be possible in the white-box setting, with full access to the DNN, e.g., [28, 57, 58, 59, 60], as well as in the black-box setting, without access to DNN weights and gradients, e.g., [61, 62, 63, 64]. Such attacks are also transferable between models [65] and can be applied in the physical world [66, 67]. Obtaining robustness against adversarial inputs is challenging, recent work focuses on achieving certified/provable robustness [68, 69, 70, 71] and variants of adversarial training [72, 73, 28], i.e., training on adversarial inputs generated on-the-fly. Adversarial training has been shown to work well empirically, and flaws such as reduced accuracy [74, 75] or generalization to attacks not seen during training has been addressed repeatedly [76, 77, 45, 78, 79]. Adversarial inputs have also been considered for quantized DNNs [80]. Corrupted inputs, in contrast, consider “naturally” occurring corruptions to which robustness/invariance is desirable for practical applications. Popular benchmarks such as MNIST-C [81], Cifar10-C or ImageNet-C [82] promote research on corruption robustness by extending standard datasets with common corruptions, e.g., blur, noise, saturation changes etc. It is argued that adversarial robustness, and robustness to random corruptions is related. Approaches are often similar, e.g., based on adversarial training [45, 83, 84]. In contrast, we consider random and adversarial bit errors in the weights, not the inputs. Nevertheless, our adversarial bit error training is similar to adversarial training.

Fault Tolerance: Fault tolerance, describes structural changes such as removed units, and has been studied in early works such as [26, 27]. These approaches obtain fault tolerant NNs using approaches similar to adversarial training [27, 26, 85]. Recently, weight dropping regularization [86] or GAN-based training [87] has been explored. Additionally, fault tolerance of adversarially robust models has been considered in [88]. We refer to [89] for a comprehensive survey. In contrast to such works, we do *not* consider structural changes/errors in DNNs.

Backdooring: The goal of backdooring is to introduce a backdoor into a DNN, allowing to control the classification result by fixed input perturbations at test time. This is usually achieved through data poisoning [90, 91, 92]. However, some works also consider directly manipulating the weights [29, 30]. However, such weight perturbations are explicitly constructed not to affect accuracy on test examples without backdoor. In contrast, we consider random or adversarial bit errors (i.e., weight perturbations) that degrade accuracy significantly.

Quantization: Due to their high applicability, efficient architectures [93, 94, 95], compression of DNN weights [96, 97] and DNN quantization, see [98], received considerable attention. While compression mainly focuses on reducing space requirements, quantization is usually motivated by more efficient DNN inference, e.g., through fixed-point quantization and arithmetic [31, 32, 33]. To avoid reduced accuracy, quantization is considered during training [18, 99], enabling low-bit quantization such as binary DNNs [37, 100]. Some works also consider quantizing activations [37, 38, 39] or gradients [40, 101, 42]. Finally, works such as [17, 18, 19, 20] study the robustness of DNNs against quantization, however, not on bit-level. Following common practice in DNN accelerators [13], we use a deterministic fixed-point quantization for training and evaluation (i.e., injecting bit errors).

D Bit Errors in Quantized DNN Weights

We provide a more detailed discussion of the considered error models: random bit errors, induced through low-voltage operation of SRAM or DRAM commonly used on DNN accelerators [12, 15]; and adversarial bit errors, motivated through attacks on accelerator memory [9].

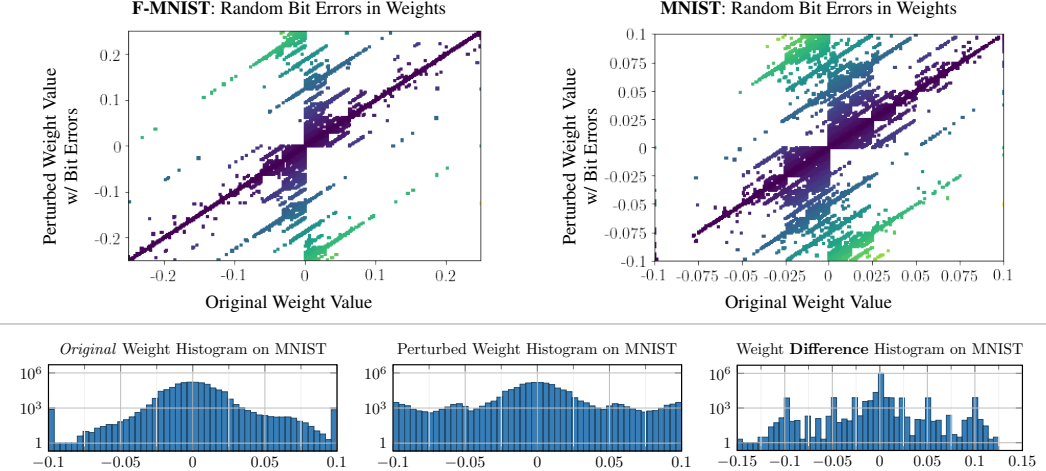


Figure 4: **Impact of Random Bit Errors.** *Top:* Original, clean weight values plotted against the perturbed weight values, i.e., after injecting random bit errors of probability $p = 1\%$. Shown are 1M weights on F-MNIST and MNIST. On F-MNIST, weights are clipped to $[-0.25, 0.25]$; on MNIST $[-0.1, 0.1]$ is used as quantization range. Color indicates the absolute error where **violet** on the diagonal means zero error and **yellow** means an error of roughly 0.375 on F-MNIST and roughly 0.15 on MNIST. *Bottom:* Histograms for the original, clean weights (left), the perturbed weights after applying random bit errors with rate $p = 1\%$ (middle) and the corresponding differences (right). The y-axis are in log-scale and a total of 1M weights are used. Note that, due to clipping in $[-0.1, 0.1]$, clean weights exhibit peaks at the boundaries.

D.1 Fixed-Point Quantization of Weights

We consider a simple *fixed-point quantization* of the floating point weights $w \in [-w_{\max}, w_{\max}]$. The range $[-w_{\max}, w_{\max}]$ is quantized using m bits into bins of width

$$\Delta = \frac{w_{\max}}{2^{m-1} - 1} \quad (7)$$

where w_{\max} is the maximum absolute weight that can be chosen based on the a pre-trained model or pre-determined. In our case, as we train *with* quantization, we pre-determine w_{\max} and additionally reduce it aggressively to improve robustness against bit errors as discussed in Sec. E.2. The quantized weights $v := Q(w)$ are signed m -bit integers (in two's complement representation) corresponding to the underlying bits. The quantization function $Q : \mathbb{R} \mapsto \{-2^{m-1}, \dots, 2^{m-1} - 1\}$ is defined as

$$Q(w) = \left\lfloor \frac{\max(-w_{\max}, \min(w_{\max}, w))}{\Delta} \right\rfloor \quad \text{and} \quad Q^{-1}(v) = v \cdot \Delta \quad (8)$$

Note that quantization includes clipping the weights to $[-w_{\max}, w_{\max}]$ before quantization. Thus, by construction, $Q^{-1}(Q(w_i)) \in [-w_{\max}, w_{\max}]$.

D.2 Low-Voltage Bit Errors

Work such as [13, 15] model the effect of low-voltage induced bit errors using two parameters: the probability p_{flt} of bit cells in accelerator memory, e.g., SRAM or DRAM, being faulty and the probability p_{err} that a faulty bit cell results in a bit error on access. Following measurements in works such as [11, 12], we assume that these errors are *not* transient errors by setting $p_{\text{err}} = 100\%$ such that the overall probability of bit errors is $p := p_{\text{flt}} \cdot p_{\text{err}} = p_{\text{flt}}$. In doing so, we consider the worst-case where faulty bit cells *always* induce bit errors. However, the noise model from the main paper remains valid for any arbitrary but fixed $p_{\text{err}} \neq 100\%$. For the remainder of this document, we assume the probability of bit error $p = p_{\text{flt}}$, with $p_{\text{err}} = 100\%$, as in the main paper. In the following, we describe the two parameters, p_{flt} and p_{err} , in more details.

Faulty Bit Cells. Due to variations in the manufacturing process, SRAM bit cells become more or less vulnerable to low-voltage operation. For a specific voltage, the resulting bit cell failures can be

SimpleNet on (F-)MNIST		SimpleNet on CIFAR10		p and ϵ on (F-)MNIST	
Layer	Output Size N_C, N_H, N_W	Layer	Output Size N_C, N_H, N_W	p in %	$\epsilon := \lceil pmW \rceil$
Conv+GN+ReLU	32, 28, 28	Conv+GN+ReLU	64, 32, 32	Random Bit Errors	
Conv+GN+ReLU	64, 28, 28	Conv+GN+ReLU	128, 32, 32	1.5	259879
Conv+GN+ReLU	64, 28, 28	Conv+GN+ReLU	128, 32, 32	1	173253
Conv+GN+ReLU	64, 28, 28	Conv+GN+ReLU	128, 32, 32	0.5	86627
Pool	64, 14, 14	Pool	128, 16, 16	0.1	17326
Conv+GN+ReLU	64, 14, 14	Conv+GN+ReLU	128, 16, 16	0.05	8663
Conv+GN+ReLU	64, 14, 14	Conv+GN+ReLU	128, 16, 16	Adversarial Bit Errors	
Conv+GN+ReLU	128, 14, 14	Conv+GN+ReLU	256, 16, 16	0.05	8631
Pool	128, 7, 7	Pool	256, 8, 8	0.01	1727
Conv+GN+ReLU	256, 7, 7	Conv+GN+ReLU	256, 8, 8	0.005	864
Conv+GN+ReLU	1024, 7, 7	Conv+GN+ReLU	256, 8, 8	0.001	173
Conv+GN+ReLU	128, 7, 7	Pool	256, 4, 4	p and ϵ on CIFAR10	
Pool	128, 3, 3	Conv+GN+ReLU	512, 4, 4	p in %	$\epsilon := \lceil pmW \rceil$
Conv+GN+ReLU	128, 3, 3	Pool	512, 2, 2	Random Bit Errors	
Avg Pool	128, 1, 1	Conv+GN+ReLU	2048, 2, 2	1	879741
FC	10	Conv+GN+ReLU	256, 2, 2	0.5	439871
W , fixed GN	1,078,794	Pool	256, 1, 1	0.1	87975
W , learnable GN	1,082,826	Conv+GN+ReLU	256, 1, 1	0.05	43988
		FC	10	Adversarial Bit Errors	
		W , fixed GN	5,489,290	0.001	879
		W , learnable GN	5,498,378	0.0005	440
				0.0001	88

Table 4: **Architectures, Number of Weights W , Number of Bit Errors ϵ . Left and Middle:** SimpleNet architectures used for MNIST/F-MNIST and CIFAR10 with the corresponding output sizes, channels N_C , height N_H and width N_W , and the total number of weights W . For NORMAL and RANDBET, we use group normalization with learnable scale/bias. For ADVBET, we found that fixing scale/bias provides improved robustness. **Right:** The number of expected bit errors for random bit errors, i.e., pmW , and the maximum number of bit errors for adversarial bit errors $\epsilon := \lceil pmW \rceil$. Here, $m = 16$ is the number of bits per weight value.

assumed to be random and independent of each other. We assume a bit to be faulty with probability p_{flt} increasing exponentially with decreased voltage [6, 11, 12, 13]. Furthermore, the faulty bits for $p'_{\text{flt}} \leq p_{\text{flt}}$ can be assumed to be a subset of those for p_{flt} [11]. For a fixed chip, consisting of multiple memory arrays, the faulty cells are pre-determined through the manufacturing process, i.e., the pattern (spatial distribution) of faulty cells is fixed for a specific supply voltage. Across chips/memory arrays, however, faulty cells are assumed to be random and independent of each other.

Bit Errors in Faulty Bit Cells: Faulty cells may cause bit errors with probability p_{err} upon read/write access. We note that bit errors read from memory affect *all* computations performed on the read weight value. We assume that a bit error flips the currently stored bit, where flips 0-to-1 and 1-to-0 are assumed equally likely.

Illustration: The impact of random bit errors on quantized weights is illustrated in Fig. 4 (top) on F-MNIST and MNIST for bit error rate $p = 1\%$. Here, the diagonal in **violet** represents zero error (i.e., no bit errors) while large absolute errors are depicted in **yellow**. For $p = 1\%$, the majority of the roughly 1M weights are not affected by bit errors. Additionally, the separation between positive and negative weights is clearly visible: bit errors not affecting the most significant bit (MSB) do not change the sign. Nevertheless, few bit errors can easily induce large errors, as shown in the weight difference histogram, Fig. 4 (bottom right): many weight values are changed by more than half of the quantization range, i.e., absolute errors of at least w_{max} . Overall, random bit errors result in a unique error pattern, significantly different from Gaussian, L_p or quantization errors studied in related work [16, 21, 17, 18, 19, 20].

Random Bit Errors on MNIST						Random Bit Errors on F-MNIST						Random Bit Errors on CIFAR10					
Training		Err	Loss	avg RErr in %		Training		Err	Loss	avg RErr in %		Training		Err	Loss	avg RErr in %	
p=1%	w_{\max}	in%	\mathcal{L}	$p=0.1$	p=1	p=1%	w_{\max}	in%	\mathcal{L}	$p=0.1$	p=1	p=1%	w_{\max}	in%	\mathcal{L}	$p=0.1$	p=1
NORMAL	1	0.36	0.02	89.92	89.98	NORMAL	1	5.37	0.21	91.04	90.85	NORMAL	1	8.32	0.38	90.84	90.81
NORMAL	0.25	0.37	0.01	89.92	90.06	NORMAL	0.5	5.53	0.22	90.36	90.81	NORMAL	0.25	8.67	0.38	18.40	91.01
NORMAL	0.1	0.29	0.34	3.71	68.67	NORMAL	0.25	5.58	0.20	88.67	90.71	NORMAL	0.15	8.13	0.34	11.32	88.99
NORMAL	0.05	0.29	1.64	1.30	22.37	NORMAL	0.2	6.26	0.22	81.33	90.17	NORMAL	0.1	8.81	0.68	11.07	75.68
RANDBET	1	0.63	0.02	90.16	90.12	RANDBET	1	10.24	0.29	42.33	47.54	RANDBET	1	9.02	0.39	86.20	90.88
RANDBET	0.1	0.31	0.35	0.45	0.62	RANDBET	0.25	7.26	0.19	9.63	11.67	RANDBET	0.15	8.89	0.33	10.17	16.08
RANDBET	0.05	0.37	1.64	0.52	0.69	RANDBET	0.2	6.76	0.19	8.99	10.78	RANDBET	0.1	8.56	0.70	9.70	14.69

Table 5: **Clipping and Random Bit Errors.** Average RErr against random bit errors with rate p considering varying degrees of clipping, i.e., reducing the quantization range $[-w_{\max}, w_{\max}]$. RANDBET was trained on $p = 1\%$ (in blue). Clipping aggressively clearly improves robustness: RErr against random bit errors with $p = 0.1\%$ and $p = 1\%$ may decrease significantly. However, test error might increase for small w_{\max} (in red) and confidences might be constrained, as seen in an increased cross-entropy loss \mathcal{L} on test examples (also red).

D.3 Adversarial Bit Errors

As introduced in the main paper, our adversarial bit error attack can be formulated as the following optimization problem on a fixed mini-batch of examples $\{(x_b, y_b)\}_{b=1}^B$:

$$\max_{\tilde{v}} \sum_{b=1}^B \mathcal{L}(f(x_b; Q^{-1}(\tilde{v})), y_b) \quad \text{s.t.} \quad d_H(\tilde{v}, v) \leq \epsilon, \quad d_H(\tilde{v}_i, v_i) \leq 1 \quad (9)$$

where \tilde{v} are the quantized weights (signed m -bit integers) and d_H denotes the (bit-level) Hamming distance. The total number of bit errors $d_H(\tilde{v}, v)$ is constrained by $\epsilon := \lceil pmW \rceil$ for a bit error rate p , and we allow at most one bit error per weight value, i.e., $d_H(\tilde{v}_i, v_i) \leq 1$. These constraints are enforced through projection, after iteratively computing:

$$\tilde{w}^{(t+1)} = \tilde{w}^{(t)} + \gamma \Delta^{(t)} \quad \text{with} \quad \Delta^{(t)} = \sum_{b=1}^B \mathcal{L}(f(x_b; \tilde{w}_q^{(t)}), y_b), \quad \tilde{w}_q^{(t)} = Q^{-1}(Q(\tilde{w}^{(t)})) \quad (10)$$

where γ is the step size. We note that the forward pass is performed on the de-quantized weights $\tilde{w}_q^{(t)} = Q^{-1}(Q(\tilde{w}^{(t)}))$, while the update is performed in floating point.

The projection after the update of Eq. (10) requires solving the following optimization problem:

$$\min_{\tilde{v}'} \|Q^{-1}(\tilde{v}) - Q^{-1}(\tilde{v}')\|_2^2 \quad \text{s.t.} \quad d_H(v_i, \tilde{v}'_i) \leq 1, \quad d_H(v, \tilde{v}') \leq \epsilon \quad (11)$$

where we dropped the superscript t for simplicity. Here, $\tilde{v} = Q(\tilde{w})$ are the quantized, perturbed weights after Eq. (10) and $\tilde{v}' = Q^{-1}(\tilde{v}')$ will be the projected weights. As the objective and the constraint set are separable, this problem can be divided into the following two problems: First, we rank the weights by their corresponding changes

$$|Q^{-1}(Q(w_i)) - Q^{-1}(\tilde{v}_i)| = |w_{q,i} - \tilde{w}_{q,i}| \quad (12)$$

where w are the original, clean weights and w_q the corresponding de-quantized weights. Then, only the top- ϵ changes are kept. All other perturbed weights $\tilde{w}_{q,i}$ are reset to the original, clean weights $w_{q,i}$. For the selected weights, only the most significant changed bit is kept. In practice, considering \tilde{v}_i and v_i from Eq. (11) corresponding to one of the top- ϵ changes, if $d_H(\tilde{v}_i, v_i) > 1$, only the highest changed bit is kept. In practice, this can be implemented (and parallelized) easily on the signed m -bit integers \tilde{v}_i and v_i while computing the (bit-level) Hamming distance d_H .

The optimization problem Eq. (9) is challenging due to the non-convex constraint set that we project onto after each iteration. Therefore, we use several random restarts, each initialized by randomly selecting $k \in [0, \epsilon]$ bits to be flipped in v to obtain $\tilde{v}^{(0)}$. We note that initialization by randomly flipping bits is important as, without initialization, i.e., $\tilde{v}^{(0)} := w$, the loss \mathcal{L} in Eq. (9) will be close to zero. We also found that initializing with $k = \epsilon$ leads to difficulties in the first few iterations, which is why we sample $k \in [0, \epsilon]$ uniformly. Additionally, we normalize the gradient $\Delta^{(t)}$ in Eq. (10) following [44]:

$$\bar{\Delta}^{(t)} = \frac{\Delta^{(t)}}{\|\Delta^{(t)}\|_1}, \quad \hat{\Delta}^{(t)} = \frac{\bar{\Delta}^{(t)}}{\max_i |\bar{\Delta}^{(t)}|} \quad (13)$$

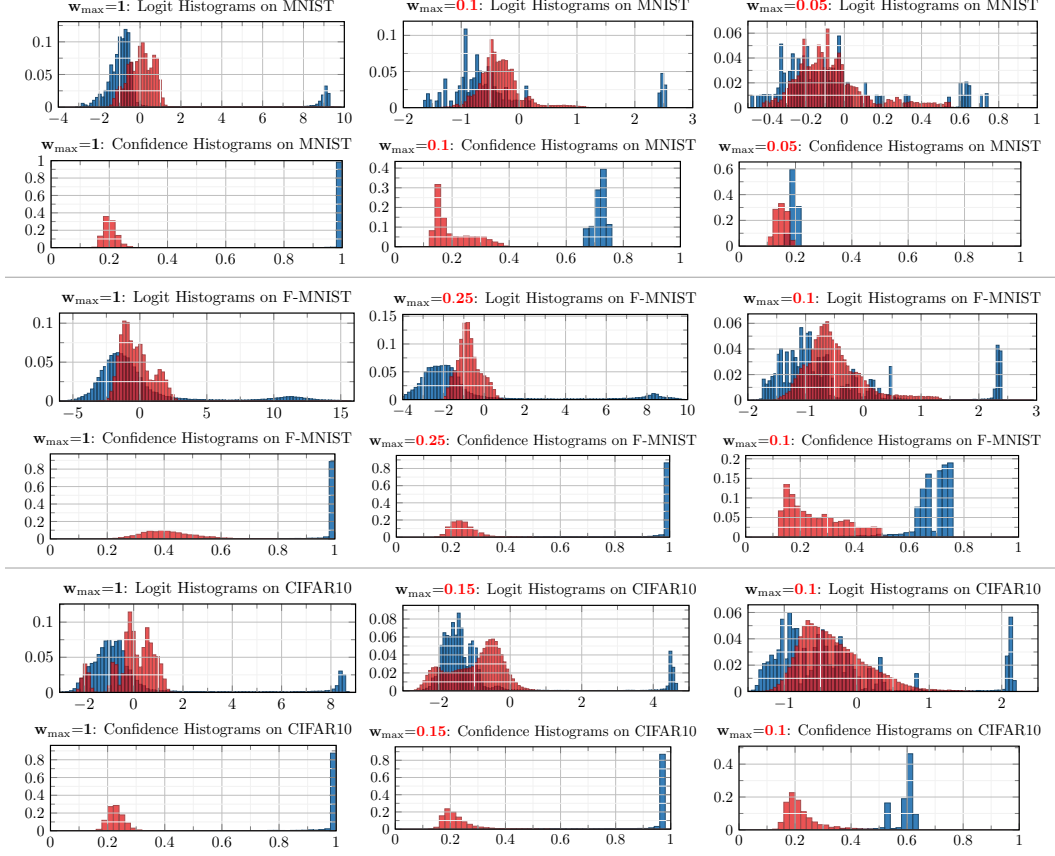


Figure 5: Impact of Clipping on Logits and Confidences. We plot *normalized* logit and confidence histograms where the confidence is $\max_k f_k(x; w)$, i.e., the maximum predicted probability, and we plot *normalized* histograms. For logits, we plot *all* logits, resulting in bi-modal histograms. We considered 5000 test examples. In **blue**, we show confidence/logits on *clean*, unperturbed weights; in **red**, we plot confidence/logits on perturbed weights (i.e., with bit errors). On MNIST, for example, we use $w_{\max} = 0.1$ for our experiments. This is justified by the significantly reduced confidences for $w_{\max} = 0.05$, even though $w_{\max} = 0.05$ could potentially increase robustness further.

before applying the update, i.e., $\tilde{w}^{(t+1)} = \tilde{w}^{(t)} + \gamma \hat{\Delta}^{(t)}$. Additionally, we apply backtracking [45]: Using an additional forward pass in each iteration, we evaluate whether $\tilde{w}^{(t+1)}$ actually increases the cross-entropy loss \mathcal{L} *after* projection compared to the previous iterate $\tilde{w}^{(t)}$. The update is kept, only if this is the case. Otherwise, $\tilde{w}^{(t+1)}$ is rejected and the step size γ is divided by $\beta > 1$. Finally, instead of considering $\tilde{w}^{(T)}$, i.e., the perturbed weights after exactly T iterations, we use

$$\tilde{w}^{(t^*)} \quad \text{with} \quad t^* = \operatorname{argmax}_t \sum_{b=1}^B \mathcal{L}(f(x_b; \tilde{w}_q^{(t)}), y_b) \quad (14)$$

instead. Nevertheless, despite these optimization tricks, the attack remains very sensitive to hyperparameters, especially regarding the step-size. Thus, in practice, we use varying step sizes, with or without gradient normalization and backtracking and use several random restarts.

E Experiments

In the following, for reproducibility, we discuss our experimental setup in more detail. Subsequently, we include additional experiments regarding clipping, batch normalization, baselines as well as random and adversarial bit error training.

Random Bit Errors with BN on MNIST				F-MNIST				CIFAR10			
Training, p in %	Err in %	RErr in %		Err	RErr in %	RErr in %		Err	RErr in %	RErr in %	
		$p = 0.5$	$p = 1.5$		$p = 0.1$	$p = 0.5$			$p = 0.1$	$p = 0.5$	
NORMAL (GN)	0.29	3.71 ± 4.53	88.74 ± 2.78	5.58	12.34 ± 1.88	88.67 ± 2.14		8.13	11.32 ± 0.32	51.13 ± 7.91	
RANDBET (GN)	0.30	0.41	0.04	0.69	0.14	9.57	0.62	8.23	9.63 ± 0.17	13.17	0.49
NORMAL BN	0.33	86.49 ± 5.58	90.05 ± 1.45	5.61	57.65 ± 15.7	90.70 ± 1.63		6.72	17.05 ± 3.22	88.92 ± 1.66	
RANDBET BN	0.39	0.72 ± 0.14	9.74 ± 11.8	5.63	8.20 ± 0.67	20.94 ± 7.26		6.27	8.69	24.96 ± 5.84	
NORMAL ResNet	0.38	60.24 ± 17.1	89.06 ± 2.15	6.20	35.72 ± 11.4	88.08 ± 3.04		7.86	14.13 ± 1.16	69.24 ± 7.13	
RANDBET ResNet	0.30	1.05 ± 0.86	26.00 ± 19.4	6.38	9.12 ± 1.02	39.42 ± 15.5		7.26	10.46 ± 1.16	25.29 ± 5.48	

Table 6: **Random Bit Errors with Batch Normalization (BN) and ResNets.** We report Err, the robust cross-entropy loss \mathcal{L} (i.e., *with* bit errors) and RErr for normal training and random bit error training (RANDBET) with various configurations of BN [50] (in red) and architectures. We consider SimpleNet with group normalization (GN) [49] or BN and ResNets [51] with BN (also in red): ResNet-20 on MNIST/F-MNIST and ResNet-34 on CIFAR10. RANDBET is trained using $p = 1.5\%$ on MNIST and $p = 0.5\%$ on F-MNIST/CIFAR10 (marked in blue). As can be seen, using BN or ResNets, which are dependent on BN for reliable training [52], results in considerably worse RErr in all cases.

E.1 Experimental Setup

Datasets: We conduct experiments on MNIST¹ [23], Fashion-MNIST² (F-MNIST) [24] and CIFAR10³ [25]. MNIST consists of 60k training and 10k test images. These are gray-scale and of size 28×28 pixels. Similarly, F-MNIST consists of 60k training and 10k test images of size 28×28 pixels. Finally, CIFAR10 consists of 50k training and 10k test images of size $32 \times 32 \times 3$ (i.e., color images). All three datasets represent classification tasks with 10 classes.

Architecture: The used SimpleNet architectures [47] for MNIST/F-MNIST and CIFAR10 are summarized in Tab. 4, including the total number of weights W . On CIFAR10, this results in a total of roughly $W \approx 5.5\text{M}$ weights. Due to the lower resolution on MNIST and F-MNIST, channel width in each convolutional layer is halved, and one stage of convolutional layers including a pooling layer is skipped. This results in a total of roughly $W \approx 1\text{M}$ weights. In both cases, we replaced batch normalization (BN) [50] with group normalization (GN) [49]. The learnable scale/bias parameters of group normalization make up for less than $10k \approx 0.16\% \cdot W$ of the weights on CIFAR10. Tab. 4 also includes the expected/maximum number of bit errors given various rates p for random/adversarial bit errors. Regarding the number of weights W , SimpleNet compares favorably to, e.g., VGG [48]: VGG-16 has 14M weights on CIFAR10. Additionally, we found SimpleNet to be easier to train without BN, which is desirable as BN reduces robustness to bit errors significantly, cf. Sec. E.3. This is also the reason why we do not use ResNets [51], which depend strongly on BN [52].

Training: For training, we use stochastic gradient descent in order to minimize cross-entropy loss, with batch size 100, learning rate 0.01, momentum 0.9, weight decay 0.0005 and learning rate decay of 0.98 for 100, 150 and 200 epochs on MNIST, F-MNIST and CIFAR10, respectively. Initialization follows [102]. We implemented architectures and training in PyTorch⁴ [103]. On all datasets, the full training set is used for training and we do not use early stopping. For **adversarial bit error training (ADVBET)**, we reduce the learning rate to 0.005, clip gradients to $[-0.05, 0.05]$, and disable learnable scale/bias in GN. We randomize the step size γ in Eq. (9) over $\{0.1, 1, 3\}$ and also randomize over backtracking and gradient normalization (i.e., with or without). As for **random bit error training (RANDBET)**, we start injecting bit errors whenever the loss reduced below 1.75.

Random Bit Errors: Following Sec. D.2, we simulate 50 different chips with multiple memory arrays, by drawing uniform samples $u^{(c)} \sim U(0, 1)^{W \times m}$ for each chip c and all m bits for a total of W weights. Then, for chip c , bit j in weight w_i is flipped iff $u_{ij}^{(c)} \leq p$. This assumes a linear memory layout of all W weights. The pattern, i.e., spatial distribution, of bit errors for chip c is fixed by $u^{(c)}$, while across all 50 chips, bit errors are uniformly distributed. We emphasize that we pre-determine $u^{(c)}$, $c = 1, \dots, 50$, once for all our experiments. Thus, our robustness results are

¹<http://yann.lecun.com/exdb/mnist/>

²<https://github.com/zalandoresearch/fashion-mnist>

³<https://www.cs.toronto.edu/~kriz/cifar.html>

⁴<https://pytorch.org/>

Fixed Bit Error Pattern on MNIST				F-MNIST			CIFAR10		
Training, p_{flt} in % ($p_{\text{err}}=100\%$)	Err in %	RErr in %		Err in %	RErr in %		Err in %	RErr in %	
		$p_{\text{flt}}=0.1$	$p_{\text{flt}}=1$		$p_{\text{flt}}=0.1$	$p_{\text{flt}}=1$		$p_{\text{flt}}=0.1$	$p_{\text{flt}}=1$
PATTBET, $p_{\text{flt}}=0.1$	0.37	0.53	89.76	6.22	8.16	90.81	9.27	13.64	93.08
PATTBET, $p_{\text{flt}}=1$	0.44	85.74	1.30	7.27	73.93	12.59	11.46	90.31	24.04
Random Bit Errors on MNIST				F-MNIST			CIFAR10		
Training, p_{flt} in % ($p_{\text{err}}=100\%$)	Err in %	avg RErr in %		Err in %	avg RErr in %		Err in %	avg RErr in %	
		$p=0.1$	$p=1$		$p=0.1$	$p=1$		$p=0.1$	$p=1$
PATTBET, $p_{\text{flt}}=0.1$	0.37	89.39 \pm 2.25	89.84 \pm 1.45	6.22	90.54 \pm 1.9	90.87 \pm 1.36	9.27	91.01 \pm 0.7	90.95 \pm 0.55
PATTBET, $p_{\text{flt}}=1$	0.44	88.56 \pm 1.97	90.12 \pm 1.27	7.27	88.39 \pm 2.74	90.53 \pm 1.78	11.46	90.86 \pm 0.7	91.08 \pm 0.63

Table 7: **Chip-Specific Baselines.** We consider training on a fixed pattern (PATTBET) of bit errors, corresponding to chip-specific training as in [12, 15], as briefly discussed in the main paper. We report *average* RErr against the same, fixed bit error patterns, as well as *random* bit errors. As shown, PATTBET does not generalize to lower bit error rates, e.g., when trained on $p = 1\%$ but tested against a *subset of the same bit errors* with $p = 0.1\%$ (in red), as well as completely random bit errors.

entirely comparable across all models as well as bit error rates p . The expected number of bit errors for various rates p is summarized in Tab. 4.

Adversarial Bit Errors: During evaluation, we consider the *worst-case* across step sizes 0.1, 0.5, 1, 3 and 5 with and without backtracking, $T = 20$ iterations and three random restarts; for step sizes 0.5 and 1 we additionally consider $T = 100$ iterations. This totals 14 attacks with 3 restarts, i.e., $14 \cdot 3 = 42$ individual attacks. We consider error rates $p \in \{0.0001, 0.0005, 0.001, 0.005, 0.01, 0.05\}$, where adversarial bit errors are constrained to $\epsilon := \lceil pmW \rceil$. The corresponding values for ϵ are summarized in Tab. 4. Furthermore, for $p' < p$, all attacks computed for p' are included in the evaluation of p : e.g., evaluating robustness against $p = 0.0005$ includes $2 \cdot 42$ individual attacks for $p = 0.0005$ and $p = 0.0001$. For $T = 20$ iterations, we use $\beta = 2$ for backtracking; for $T = 100$, we use $\beta = 1.5$, cf. Sec. D.3. Adversarial bit error attacks are computed, i.e., “trained”, on one mini-batch of size 100 corresponding to the last 100 test examples.

Metrics: We report (**clean**) **test error** **Err**, computed as the fraction of mis-classified test examples on *clean*, unperturbed weights, and **robust test error** **RErr**, computed as the test error on *perturbed* weights (i.e., after injecting random or adversarial bit errors). Both are computed on the first 9000 test examples of each dataset. For random bit errors, we report *average* RErr and its standard deviation in % across 50 samples of random bit errors of rate p . Regarding adversarial bit errors, we report *worst-case* RErr across all attacks, corresponding to the maximum RErr across all attacks.

Quantization: We use the fixed-point quantization outlined in Sec. D.1 using $m = 16$ bits in all our experiments, i.e., both for training and injecting random/adversarial bit errors. Bit error injecting was implemented as custom modules for PyTorch in C/CUDA and directly operates on the m -bit signed integer representation of quantized weights, i.e., $v_i = Q(w_i) \in \{2^{m-1}, \dots, 2^{m-1} - 1\}$. When using BN with quantization, as the forward pass is performed using the “de-quantized model” $w_q = Q^{-1}(Q(w))$ while the update is applied to the corresponding “floating-point model” w , the statistics need to be updated accordingly. As Eq. (8) includes clipping the weights to $[-w_{\text{max}}, w_{\text{max}}]$, this clipping needs to be applied to the floating point weights w , as well.

E.2 Clipping

In Tab. 5, we report additional results regarding more aggressive clipping, i.e., reducing w_{max} , to obtain robustness against random bit errors. Specifically, we report *average* RErr against random bit errors with probability $p = 0.1\%$ and $p = 1\%$. Complementary, Fig. 5 shows the corresponding logit and confidence histograms. As shown, clipping can improve robustness significantly: on MNIST and CIFAR10, normal training with clipping ($w_{\text{max}} = 0.05$ and $w_{\text{max}} = 0.1$, respectively) yields 1.3% and 11.07% RErr against $p = 0.1\%$. This is close to RANDBET. However, in all cases, extreme clipping leads to an increased test error (marked in red). This is supported by Fig. 5 showing reduced logits and confidences for very low w_{max} , i.e., overly aggressive clipping. This also results in a significantly higher cross entropy loss \mathcal{L} in Tab. 5. Intuitively, with extremely constrained weights, the DNN is not able to obtain large logits in order to reduce the loss during training. On more difficult datasets such as F-MNIST and CIFAR10 this leads to an increase in Err. We also found that the logits

Random Bit Errors on MNIST with $w_{\max}=0.1$									
Training, p in %	Err in%	Average RErr in %, p for evaluation in %					MSB* $p=1.5$		
		$p=0.5$	$p=1$	$p=1.5$	$p=2$	$p=2.5$			
NORMAL, $w_{\max}=1$	0.36	89.92 \pm 1.49	89.98 \pm 1.59	89.93 \pm 1.17	90.05 \pm 1.2	90.21 \pm 1.23	89.91 \pm 1.4		
NORMAL	0.29	3.71 \pm 4.53	68.67 \pm 14.6	88.74 \pm 2.78	89.54 \pm 1.53	90.02 \pm 1.08	84.02 \pm 5.81		
RANDBET, $p=0.5$	0.27	0.52 \pm 0.08	1.27 \pm 0.36	7.67 \pm 4.09	39.21 \pm 12.6	74.98 \pm 8.59	2.09 \pm 1.1		
RANDBET, $p=1$	0.31	0.45 \pm 0.05	0.62 \pm 0.1	1.03 \pm 0.23	2.44 \pm 1.4	8.85 \pm 6.48	0.75 \pm 0.14		
RANDBET, $p=1.5$	0.30	0.41 \pm 0.04	0.52 \pm 0.06	0.69 \pm 0.14	0.97 \pm 0.21	1.77 \pm 0.69	0.56 \pm 0.09		
RANDBET, $p=2$	0.34	0.47 \pm 0.03	0.55 \pm 0.05	0.66 \pm 0.1	0.83 \pm 0.14	1.16 \pm 0.33	0.57 \pm 0.06		
RANDBET, $p=2.5$	0.37	0.45 \pm 0.03	0.51 \pm 0.04	0.59 \pm 0.07	0.70 \pm 0.1	0.86 \pm 0.14	0.53 \pm 0.05		
MSBBET *, $p=1.5$	0.29	0.41 \pm 0.04	0.55 \pm 0.07	0.83 \pm 0.2	1.66 \pm 0.76	4.74 \pm 2.77	0.63 \pm 0.09		
ADVBET $_{\lambda=1}$, $p=0.01$	0.49	0.55 \pm 0.02	0.60 \pm 0.03	0.65 \pm 0.05	0.71 \pm 0.06	0.78 \pm 0.06	0.63 \pm 0.03		
ADVBET $_{\lambda=0}$, $p=0.01$	0.52	0.58 \pm 0.03	0.60 \pm 0.03	0.63 \pm 0.03	0.68 \pm 0.04	0.72 \pm 0.05	0.61 \pm 0.03		
Random Bit Errors on F-MNIST with $w_{\max}=0.25$									
Training, p in %	Err in%	Average RErr in %, p for evaluation in %					MSB* $p=1$		
		$p=0.05$	$p=0.1$	$p=0.5$	$p=1$	$p=1.5$			
NORMAL, $w_{\max}=1$	5.37	88.69 \pm 2.31	90.69 \pm 1.3	91.04 \pm 1.62	90.85 \pm 1.4	90.78 \pm 1.49	72.78 \pm 7.76		
NORMAL	5.58	8.24 \pm 0.43	12.34 \pm 1.88	88.67 \pm 2.14	90.71 \pm 1.54	90.87 \pm 1.33	90.56 \pm 1.25		
RANDBET, $p=0.05$	5.79	7.43 \pm 0.21	8.80 \pm 0.35	80.39 \pm 4.71	90.31 \pm 1.37	90.91 \pm 1.42	89.95 \pm 1.53		
RANDBET, $p=0.1$	5.57	6.83 \pm 0.17	7.73 \pm 0.31	52.51 \pm 8.49	88.46 \pm 2.09	90.44 \pm 1.32	87.47 \pm 2.67		
RANDBET, $p=0.5$	6.19	6.84 \pm 0.13	7.22 \pm 0.17	9.57 \pm 0.62	16.39 \pm 2.32	47.21 \pm 10	39.95 \pm 8.57		
RANDBET, $p=1$	7.26	7.87 \pm 0.15	8.15 \pm 0.18	9.63 \pm 0.51	11.67 \pm 1.03	15.13 \pm 1.76	13.06 \pm 1.65		
RANDBET, $p=1.5$	7.93	8.42 \pm 0.1	8.70 \pm 0.18	9.99 \pm 0.35	11.37 \pm 0.62	12.97 \pm 0.95	10.78 \pm 0.56		
MSBBET *, $p=1$	7.26	7.88 \pm 0.14	8.17 \pm 0.17	9.88 \pm 0.57	12.26 \pm 1	17.61 \pm 2.45	11.20 \pm 0.67		
ADVBET $_{\lambda=1}$, $p=0.005$	8.44	9.09 \pm 0.13	9.47 \pm 0.17	12.84 \pm 0.97	26.79 \pm 5.4	66.02 \pm 9.62	19.72 \pm 1.83		
ADVBET $_{\lambda=0}$, $p=0.005$	12.70	13.25 \pm 0.18	13.57 \pm 0.19	16.60 \pm 0.95	24.07 \pm 1.95	39.43 \pm 4.8	21.51 \pm 1.67		
Random Bit Errors on CIFAR10 with $w_{\max}=0.15$									
Training, p in %	Err in%	Average RErr in %, p for evaluation in %					MSB* $p=1$		
		$p=0.05$	$p=0.1$	$p=0.5$	$p=1$	$p=1.5$			
NORMAL, $w_{\max}=1$	8.32	90.86 \pm 0.81	90.84 \pm 0.69	90.93 \pm 0.53	90.81 \pm 0.53	90.81 \pm 0.51	77.33 \pm 4.62		
NORMAL	8.13	10.01 \pm 0.19	11.32 \pm 0.32	51.13 \pm 7.91	88.99 \pm 1.55	90.56 \pm 0.56	87.41 \pm 2.25		
RANDBET, $p=0.05$	8.04	9.83 \pm 0.18	11.04 \pm 0.34	45.84 \pm 9.67	88.52 \pm 2.22	90.70 \pm 0.74	86.60 \pm 2.84		
RANDBET, $p=0.1$	7.97	9.55 \pm 0.17	10.56 \pm 0.23	34.52 \pm 6.32	86.43 \pm 3.36	90.27 \pm 0.6	82.89 \pm 4.83		
RANDBET, $p=0.5$	8.23	9.16 \pm 0.13	9.63 \pm 0.17	13.17 \pm 0.49	20.93 \pm 1.53	40.67 \pm 4.54	17.36 \pm 1.1		
RANDBET, $p=1$	8.89	9.74 \pm 0.13	10.17 \pm 0.17	12.59 \pm 0.38	16.08 \pm 0.83	21.35 \pm 1.71	14.71 \pm 0.69		
RANDBET, $p=1.5$	9.79	10.61 \pm 0.1	10.98 \pm 0.14	13.14 \pm 0.46	15.58 \pm 0.65	18.73 \pm 0.99	14.58 \pm 0.53		
MSBBET *, $p=1$	8.51	9.37 \pm 0.14	9.75 \pm 0.14	12.37 \pm 0.46	16.74 \pm 0.98	24.12 \pm 2.29	14.53 \pm 0.7		
ADVBET $_{\lambda=1}$, $p=0.001$	10.07	11.55 \pm 0.13	12.34 \pm 0.19	22.56 \pm 2.06	60.50 \pm 8.22	84.67 \pm 4.96	44.71 \pm 5.34		
ADVBET $_{\lambda=0}$, $p=0.001$	10.79	11.95 \pm 0.08	12.50 \pm 0.11	18.24 \pm 0.91	38.99 \pm 5.58	71.72 \pm 8.1	30.59 \pm 2.98		

Table 8: **Random Bit Errors.** We report *average-case* RErr on MNIST, F-MNIST and CIFAR10, with complementary results not included in the main paper. In addition to random bit errors with rate p in %, we also evaluate against bit errors in most-significant bits (MSBs): for bit error rate p , we only keep the bit errors in MSBs, on average resulting in p/m % bit errors, where $m = 16$ is the number of bits per weight value. We also use bit errors in MSBs during training (MSBBET). RANDBET tends to increase Err with larger p . However, RANDBET does not generalize to “more” (i.e., higher p) bit errors than seen during training, creating a trade-off between RErr and Err. Also, a significant part of the RErr on random bit errors is, in fact, caused by bit errors in MSBs.

from clean, unperturbed weights and those from perturbed weights with bit errors have more overlap when clipping aggressively, e.g., for $w_{\max} = 0.05$ on MNIST.

E.3 Batch Normalization

Tab. 6 reports results for SimpleNet with group normalization (GN) [49] or batch normalization (BN) [50], as well as ResNets [51]. On MNIST and F-MNIST, we consider ResNet-20 and additionally halve the channel widths, resulting in roughly 1M weights as our SimpleNet model. On CIFAR10, we use ResNet-34, also with halved channel widths, resulting in roughly 5.3M weights. Across all datasets, using SimpleNet with BN results in considerably higher RErr against random bit errors compared to our default SimpleNet with GN. On MNIST, for example, RErr for RANDBET increases

Adversarial Bit Errors on MNIST, with $w_{\max}=0.1$							
Training, p in %	Err in %	Worst RErr in %, p for evaluation in %					
		0.0001	0.0005	0.001	0.005	0.01	0.05
NORMAL, $w_{\max} = 1$	0.36	40.47	91.07	91.07	93.68	94.08	94.08
NORMAL	0.29	0.32	62.17	91.07	91.07	91.07	91.09
RANDBET, $p = 1$	0.31	0.37	0.63	91.07	91.07	91.07	94.13
RANDBET, $p = 2.5$	0.37	0.43	0.73	88.74	91.11	91.16	91.27
ADVBET $_{\lambda=1}$, $p = 0.005$	0.32	0.33	0.48	0.67	10.39	79.43	90.24
ADVBET $_{\lambda=0}$, $p = 0.005$	0.33	0.36	0.41	0.47	1.38	89.27	89.91
ADVBET $_{\lambda=1}$, $p = 0.01$	0.49	0.59	2.81	10.18	10.54	21.43	89.86
ADVBET $_{\lambda=0}$, $p = 0.01$	0.52	0.56	1.70	3.52	10.78	11.10	89.90
ADVBET $_{\lambda=1}$, $p = 0.05$	0.54	6.21	37.67	78.72	78.72	78.72	90.26
ADVBET $_{\lambda=0}$, $p = 0.05$	22.11	32.22	54.98	60.31	61.14	74.90	93.82

Adversarial Bit Errors on F-MNIST, with $w_{\max}=0.1$							
Training, p in %	Err in %	Worst RErr in %, p for eval in %					
		0.0001	0.0005	0.001	0.005	0.01	0.05
NORMAL	5.37	71.18	91.76	91.76	94.39	94.39	
NORMAL, $w_{\max} = 1$	5.58	13.41	91.66	91.66	91.66	91.66	
RANDBET, $p = 1$	7.26	9.26	40.18	90.90	91.20	91.20	
RANDBET, $p = 1.5$	7.93	11.91	87.22	90.18	91.13	91.13	
ADVBET $_{\lambda=1}$, $p = 0.001$	6.12	7.08	7.82	70.87	91.07	91.07	
ADVBET $_{\lambda=0}$, $p = 0.001$	7.16	8.56	10.59	12.04	91.02	91.02	
ADVBET $_{\lambda=1}$, $p = 0.005$	8.44	11.84	16.39	18.06	29.86	91.33	
ADVBET $_{\lambda=0}$, $p = 0.005$	12.70	17.82	25.98	25.98	37.36	91.21	
ADVBET $_{\lambda=1}$, $p = 0.01$	6.68	8.64	12.41	15.99	66.76	91.19	
ADVBET $_{\lambda=0}$, $p = 0.01$	22.94	26.06	27.87	29.81	45.29	90.31	

Adversarial Bit Errors on CIFAR10, with $w_{\max}=0.1$							
Training, p in %	Err in %	Worst RErr in %, p for eval in %					
		0.0001	0.0005	0.001	0.005	0.01	0.05
NORMAL	8.32	91.16	93.12	93.12	93.12		
NORMAL, $w_{\max} = 1$	8.13	90.11	90.90	90.90	90.90		
RANDBET, $p = 1$	8.89	47.74	90.94	90.94	90.94		
RANDBET, $p = 1.5$	9.79	41.89	91.00	91.02	91.02		
ADVBET $_{\lambda=1}$, $p = 0.0005$	10.02	11.38	38.12	90.72	92.16		
ADVBET $_{\lambda=0}$, $p = 0.0005$	9.82	11.06	13.33	83.63	92.20		
ADVBET $_{\lambda=1}$, $p = 0.001$	10.07	11.28	20.73	63.03	90.36		
ADVBET $_{\lambda=0}$, $p = 0.001$	10.79	11.93	15.16	40.19	90.38		

Table 9: **Adversarial Bit Errors.** Worst-case RErr against adversarial bit errors. Specifically, we report the worst-case across 14 attacks per model and rate p with 3 random restarts each, resulting in a total of 42 individual attacks. We consider various hyper-parameters and up to $T = 100$ iterations, see Sec. E.3. ADVBET is able to improve robustness significantly for adversarial bit error rates p seen during training, or lower. However, it does not generalize to larger error rates. Furthermore, ADVBET proved difficult to train for large rates, e.g., $p = 0.05\%$ on MNIST or $p = 0.01\%$ on F-MNIST. Except on F-MNIST, training only on adversarial bit errors, i.e., $\lambda = 0$, results in better robustness compared to $\lambda = 1$, however, also increases Err.

from 0.69% to 9.74% against bit error rate $p = 1.5\%$ which is also used for training. On F-MNIST and CIFAR10, RErr roughly doubles for $p = 0.5\%$ (also used for training). Worse results are shown for ResNets. For example, on MNIST, RErr increases further from 9.74% to 26% RErr for $p = 1.5\%$. Overall, these experiments demonstrate that DNNs utilizing BN are significantly less robust against random bit errors, justifying our choice of using SimpleNet with GN.

E.4 Random Bit Errors

Baseline: Tab. 7 reports results of our chip-specific baselines, similar to [12, 15]. In this scenario, we fix the bit error pattern, i.e., the spatial distribution, for *both* training and evaluation. In practice, this is achieved by considering $u^{(1)}$ only, cf. Sec. E.1. We train and evaluate with $p = 0.1\%$ and $p = 1\%$ where the bit error pattern for $p = 0.1\%$ is a subset of the pattern corresponding to $p = 1\%$. As shown, **(fixed) bit error pattern training (PATTBET)** with $p = 1\%$ does *not* generalize to bit errors with rate $p = 0.1\%$, as marked in red. On MNIST, as mentioned in the main paper, RErr

is 1.3% against $p = 1\%$, but increases to 86% for $p = 0.1\%$. This is surprising as the DNN “saw” all bit errors for $p = 0.1\%$ during training. Thus, we suspect that DNNs treat fixed bit errors as “additive biases” in the corresponding weight values. For example, a bit error in the least significant bit (LSB) of a weight value results in a constant, additive bias of $\pm\Delta$, cf. Eq. (7), depending on the sign bit. As weight values do not change their sign frequently during training, this bias can be assumed fixed throughout training, allowing DNNs to overfit to particular bit error patterns. This prevents generalization to higher supply voltages, as would be necessary for, e.g., dynamic voltage scaling [13]. Tab. 7 also shows *average* RErr and its standard deviation when evaluated on random bit errors, i.e., considering all $u^{(c)}$ in Sec. E.1. It becomes apparent, that PATTBET does not generalize to random bit errors, i.e., other chips. On all datasets, RErr increases to roughly 90%, even for $p = 0.1\%$. This means that these DNNs need to be trained for specific voltages *and* chips. This, however, is clearly infeasible in practice.

Random Bit Error Training: Tab. 8 presents *average* RErr and its standard deviation (in gray) for random bit error training (RANDBET), complementing the results in the main paper. Specifically, we report results for various error rates p used for training (in **blue**) and evaluation. In **red**, we mark the RErr if RANDBET is trained *and* evaluated on the same bit error rate p . As can be seen, RANDBET provides robustness against bit error rates lower or equal to p , but generalizes poorly to significantly larger bit error rates. This is emphasized on F-MNIST and CIFAR10: for example, training with $p = 0.1\%$ on F-MNIST yields 7.73% RErr against error rate $p = 0.1\%$. However, RErr increases to 52.51% against $p = 0.5\%$ and 88.46% against $p = 1\%$. Additionally, standard deviation increases significantly. On F-MNIST and CIFAR10, Err is shown to increase quickly when training with more bit errors, i.e., higher bit error rate p . On F-MNIST, training with $p = 1.5\%$ results in 7.93% Err compared to 5.37% of a normally trained model without clipping (i.e., $w_{\max} = 1$). Emphasizing the impact of bit errors in the most-significant bits (MSBs), we also report results against random bit errors in MSBs *only*, cf. right-most column. Here, for bit error rate p , we only keep bit errors in MSBs, resulting in roughly $p/16\%$ bit errors in total. Nevertheless, for $p = 1\%$ on F-MNIST, bit errors in MSBs likely contribute most to the overall RErr: 10.78% considering only bit errors in MSBs, and 11.37% considering all, i.e., 16 times more, bit errors against RANDBET trained with $p = 1.5\%$ (marked in **bold**). Vice-versa, random MSB bit error training (MSBBET), results in surprisingly robust models even though only $1/16$ of the bit errors are seen during training. Similarly, ADVBET provides robustness against (random) bit error rates p several magnitudes larger than seen during training.

E.5 Adversarial Bit Errors

In Tab. 9, we consider the *worst-case* RErr on adversarial bit errors. We mark in **red**, if adversarial bit error training (ADVBET) with $\lambda = 0$ or $\lambda = 1$ is trained and evaluated using the same error rate p . On MNIST, we are able to train with significantly higher error rates compared to F-MNIST and CIFAR10. For example, $p = 0.01\%$ corresponds to a maximum of $\epsilon := \lceil pmW \rceil = 1727$ bit errors. However, our SimpleNet models on CIFAR10 also contain significantly more weights, such that even $p = 0.001\%$ corresponds to $\epsilon = 879$. On MNIST and F-MNIST, we show that we are not able to train ADVBET with $p = 0.05\%$ and $p = 0.01\%$, respectively. Additionally, ADVBET does not generalize to larger error rates than seen during training. Similar observations have been made using adversarial training on adversarial inputs [28]. Except for $p = 0.005\%$ on F-MNIST, training only with adversarial bit errors (ADVBET $_{\lambda=0}$) results in lower RErr compared to training both on clean and perturbed weights (ADVBET $_{\lambda=1}$). However, ADVBET $_{\lambda=0}$ increases Err significantly. This observation is also similar to training on adversarial inputs [74]. Finally, Tab. 8 shows that ADVBET is able to generalize to large error rates p , often in the order of two or three magnitudes, than seen during training as long as these errors are injected randomly. As result, ADVBET proves effective against both adversarially injected bit errors as well as adversarially reduced voltage.